



Nano Graphene Platelets (NGPs), Graphene Nanocomposites, and Graphene-Enabled Energy Devices

Bor Z. Jang

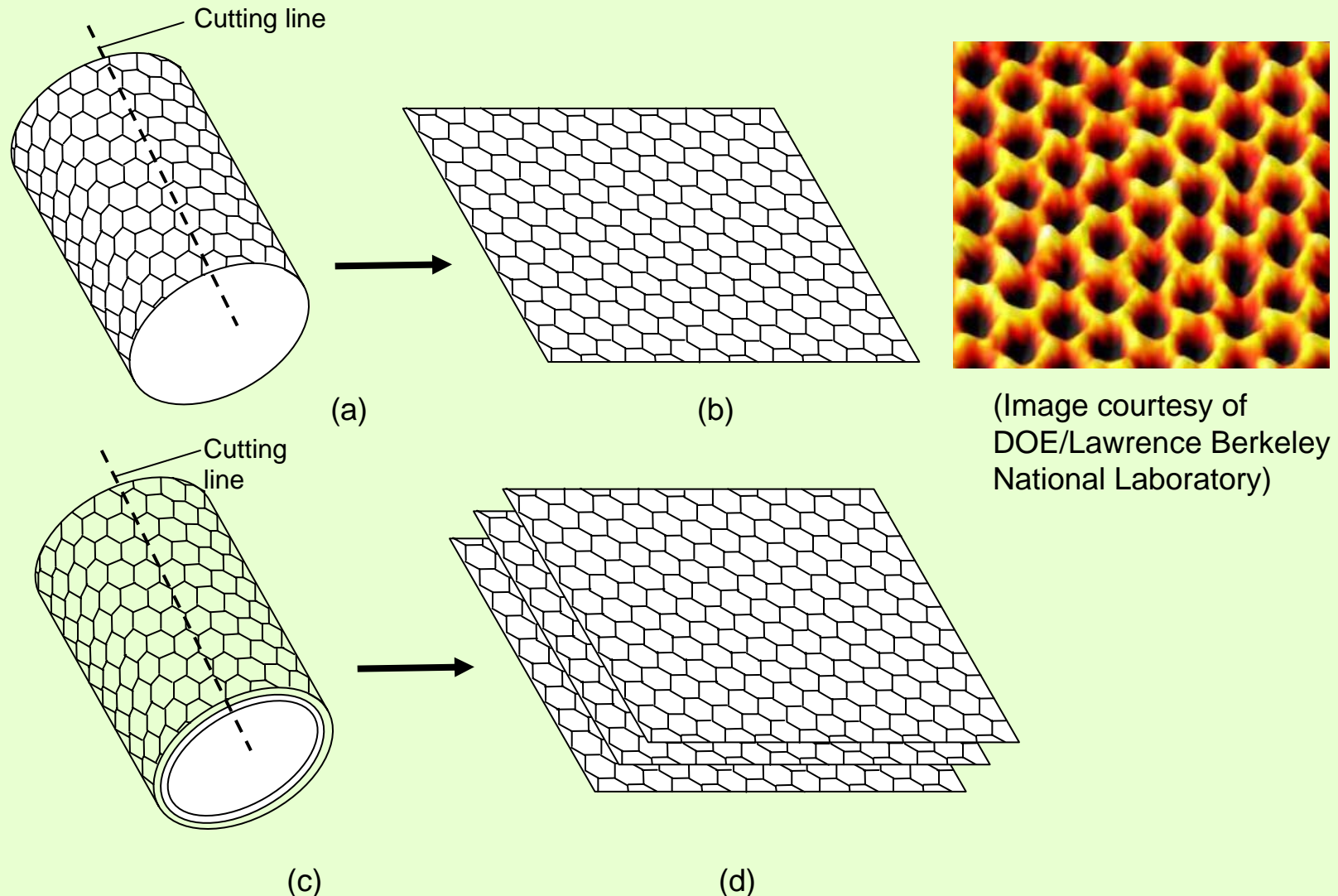
Wright State University, College of Engineering
Dayton, Ohio 45435
Bor.Jang@Wright.edu

Aruna Zhamu, President and CTO

Angstrom Materials, Inc., 1240 McCook Ave.
Dayton, Ohio 45404 Phone (937) 331-9884
Aruna.Zhamu@AngstromMaterials.com
www.AngstromMaterials.com

Outline

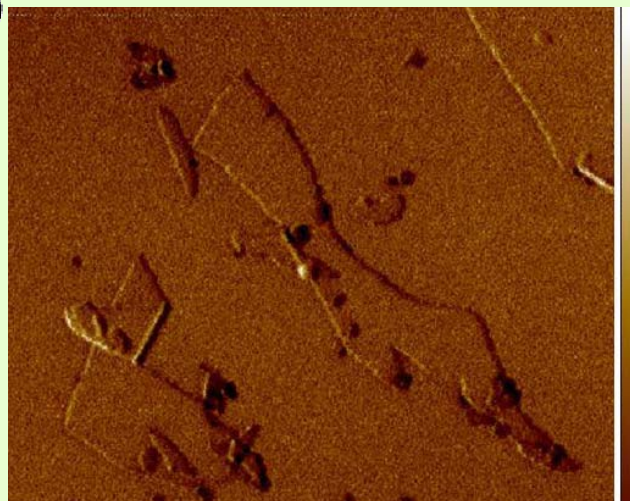
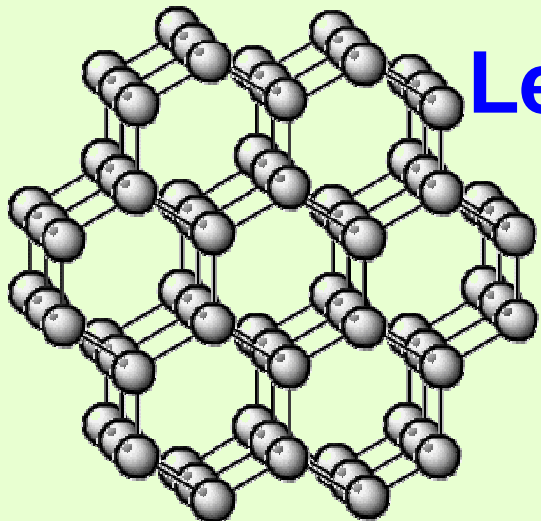
- What is a *nano graphene platelet (NGP)*?
Also known as
 - *Nano graphene sheet*,
 - *graphene nano ribbon (GNR)*,
 - *graphite nanoplatelet (GNP)*,
 - *carbon nano sheet (CNS)*, *carbon nano film*, or
carbon nano ribbon (CNR).
- How are NGPs made?
- Unique features of NGPs.
- Potential applications of NGPs.
- Current research issues.



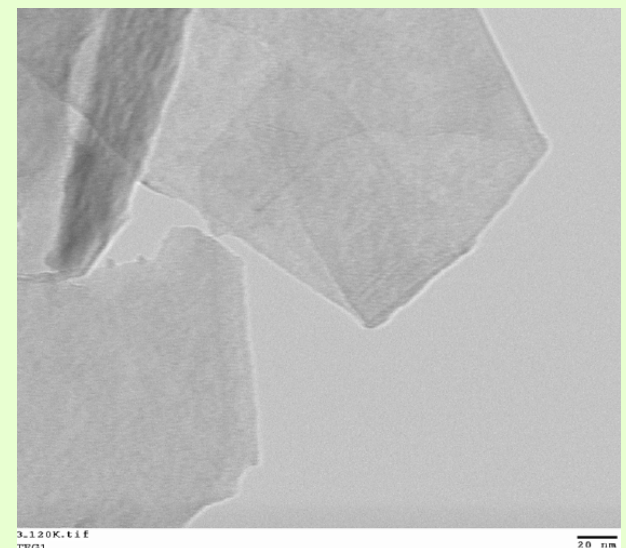
(Image courtesy of
DOE/Lawrence Berkeley
National Laboratory)

Figure 1: Conceptually, NGPs may be viewed as flattened versions of carbon nanotubes (CNTs). (a) single-wall carbon nanotube (SW-CNT); (b) a corresponding single-layer NGP; (c) multi-wall carbon nanotubes (MW-CNT); and (d) a corresponding multi-layer NGP.

NGPs:
Thickness: 0.34 – 100 nm
Length/width: 0.3- 10 μm typical

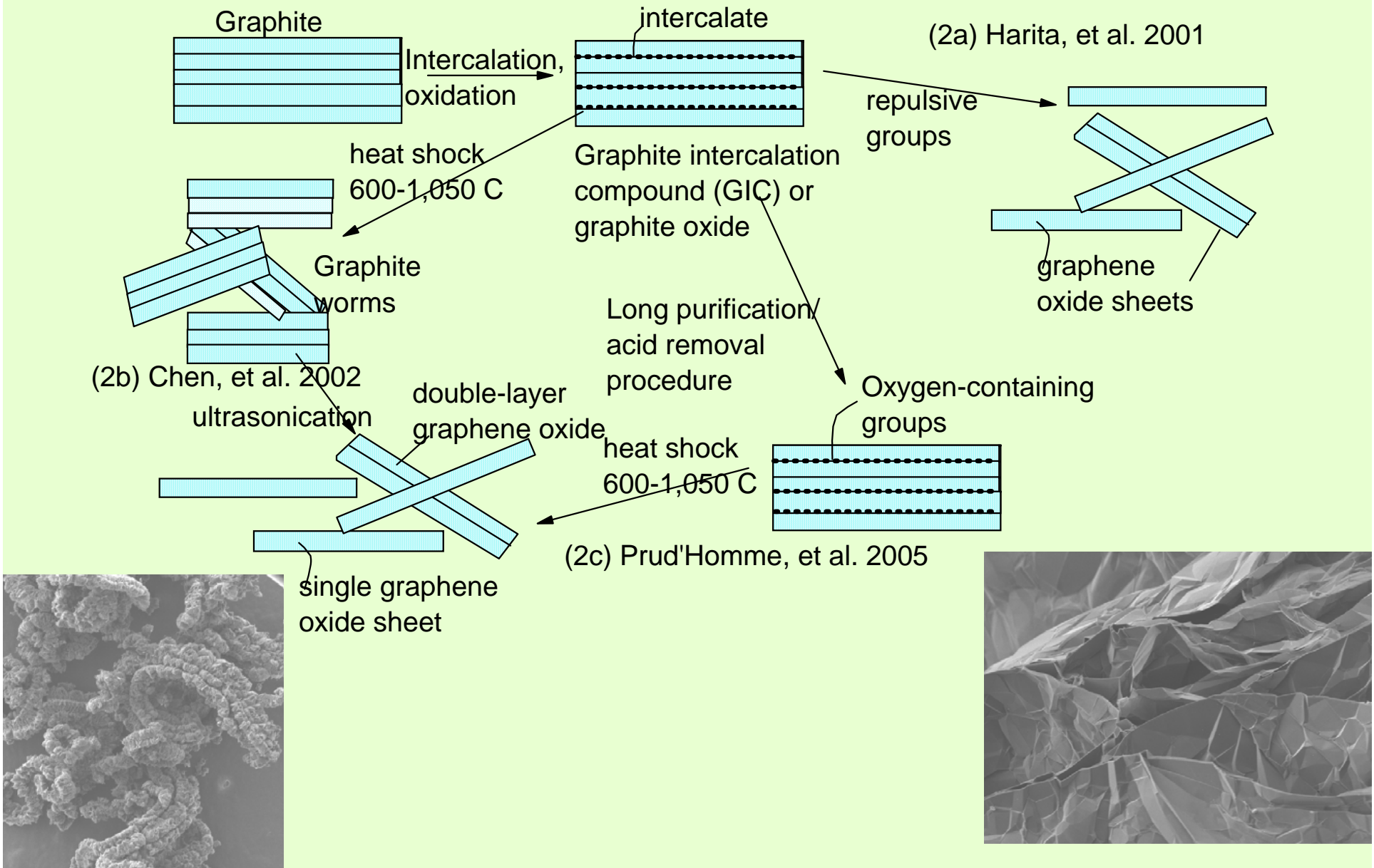


----- 100 nm



Preparation of Oxidized NGPs

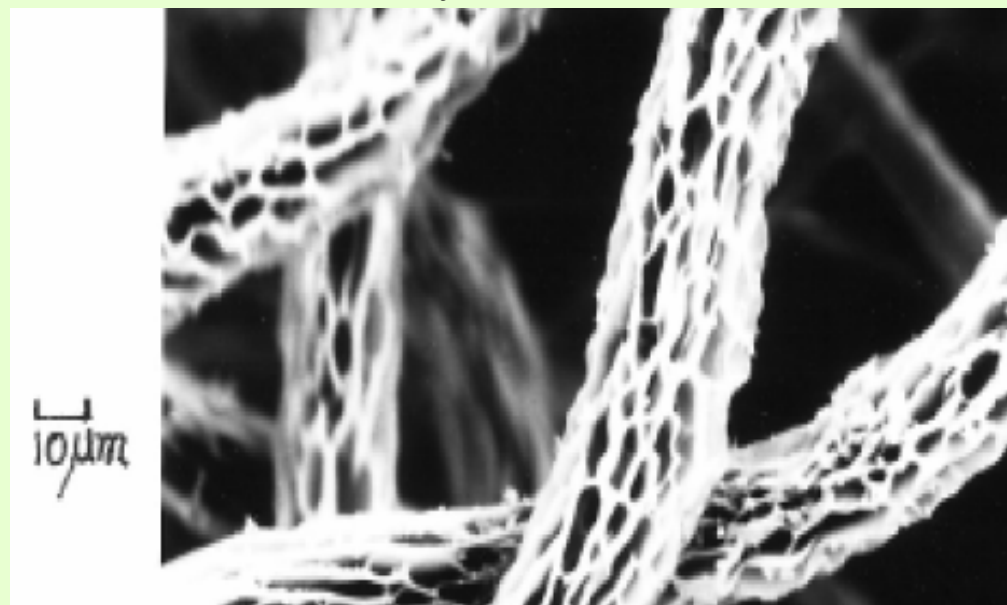
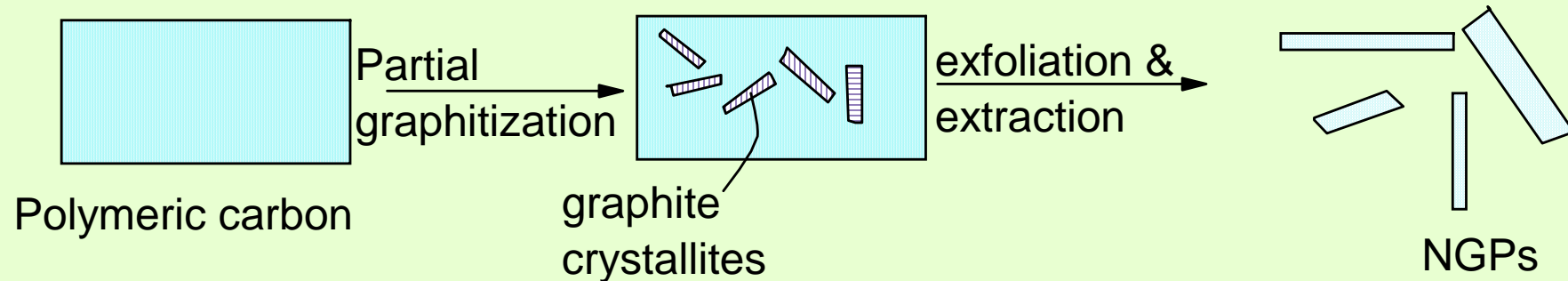
Graphite intercalation/oxidation approach



Preparation of Pristine Graphene

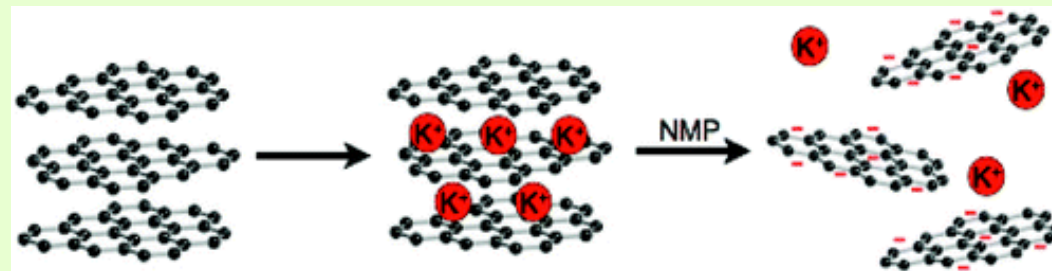
- Isolation (extraction) of ultra-thin NPGs from a carbon matrix (Jang, et al. 2002, Nanotek Instruments, Inc.) -- A Bottom-up Approach

(1) Graphene extraction (Jang, et al. 2002)



Preparation of Pristine NGPs

- K/Na/Cs Intercalation + alcohol/water-induced exfoliation (Mack, et al., 2005, UCLA)
 - with K, Na, or K/Cs eutectic melt intercalation



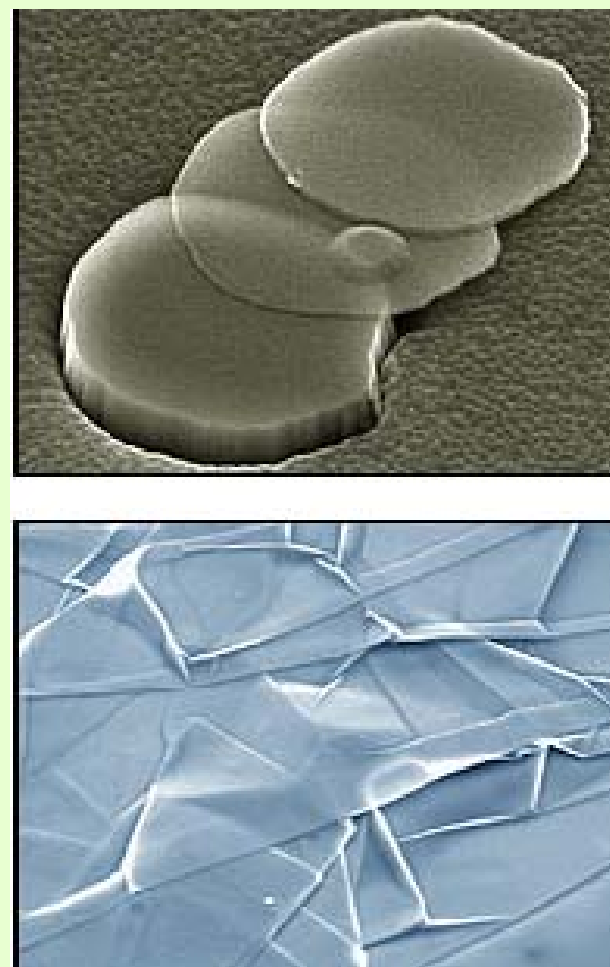
- Direct production of pristine graphene from non-oxidized and non-intercalated graphite (Zhamu and Jang, et al., 2006, Nanotek Instruments, Inc./Angstron Materials, Inc.)
 - Graphite never exposed to any obnoxious chemicals (oxidizing agents);
 - No chemical reduction necessary;

Preparation of NGPs

Peeling off using “Scotch tape” (Novoselov, et al., 2004, Univ. of Manchester).

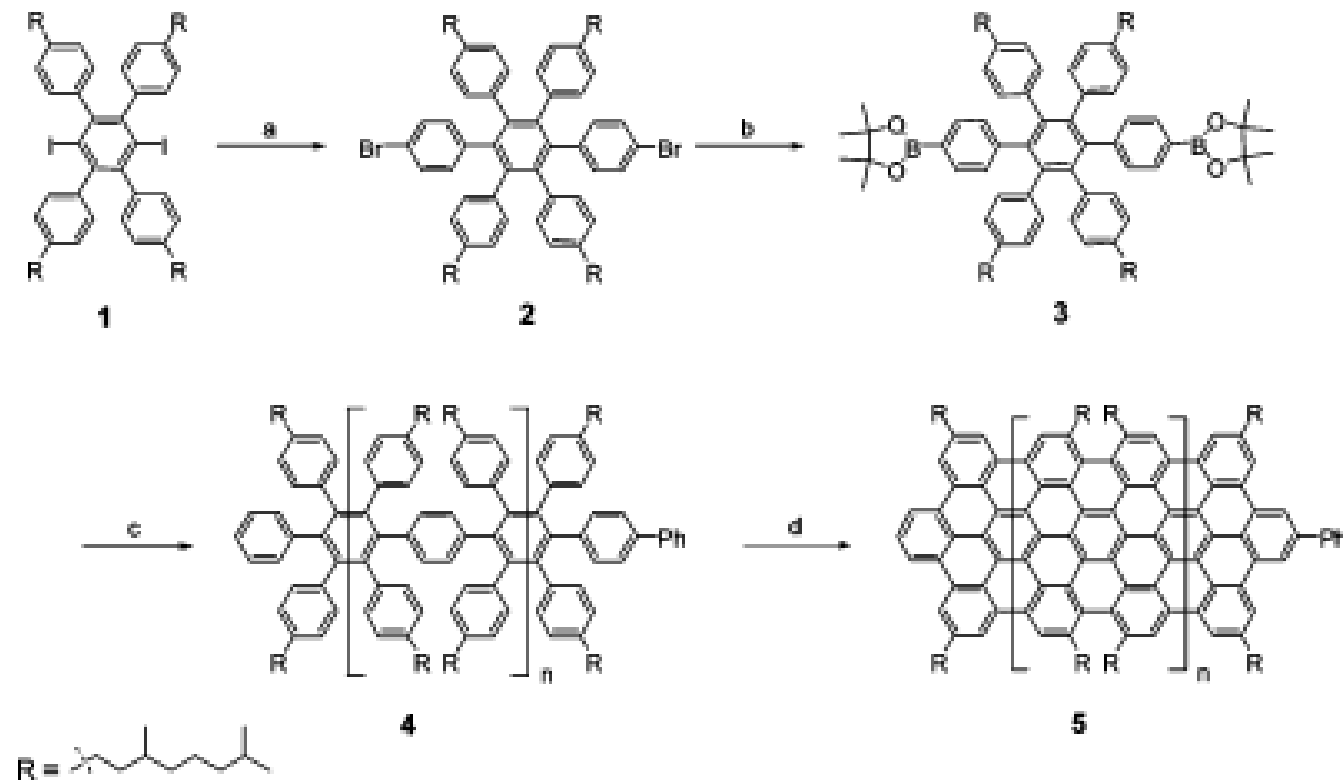


With Scotch Tape
(Dr. Lin, UC)



Bottom-up Approach (e.g., X. Yang, et al. J. Am. Chem. Soc. 2008, 130, 4216-4217)

Scheme 1. Synthesis of Graphene Nanoribbon 5^a

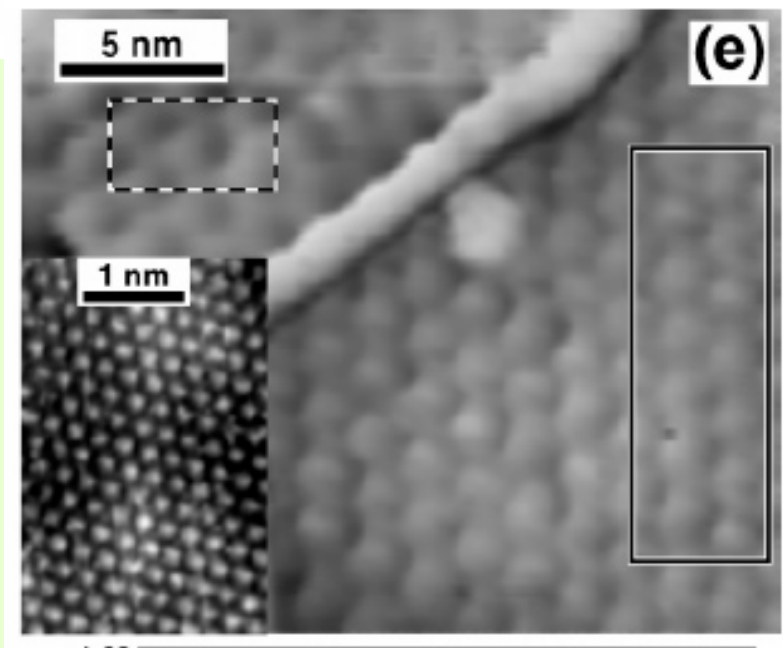
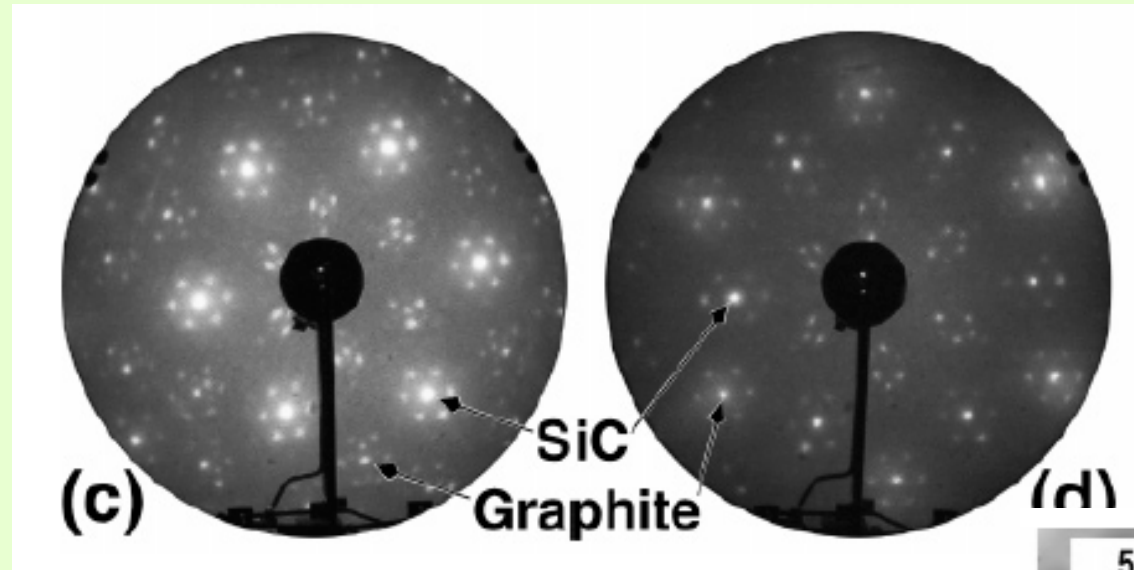


^a Reagents and conditions: (a) 4-bromophenylboronic acid, $\text{Pd}(\text{PPh}_3)_4$, aliquat 336, K_2CO_3 , toluene, 80°C , 24 h, 93%. (b) (i) $n\text{-BuLi}$, THF, -78°C , 1 h; (ii) 2-isopropoxy-4,4,5,5-tetramethyl[1,3,2]dioxaborolane, rt, 2 h, 82%. (c) compound 1, $\text{Pd}(\text{PPh}_3)_4$, aliquat 336, K_2CO_3 , toluene/ H_2O , reflux, 72 h, 75%. (d) FeCl_3 , $\text{CH}_2\text{Cl}_2/\text{CH}_3\text{NO}_2$, 25°C , 48 h, 65%.

Epitaxial Growth

e.g., Nano graphene grown epitaxially on SiC(0001);

C. Berger, et al., *J. Phys. Chem. B* 2004, 108, 19912-19916



Chemical Vapor Deposition, M. Zhu, et al., Diamond & Related Materials 16 (2007) 196–201.

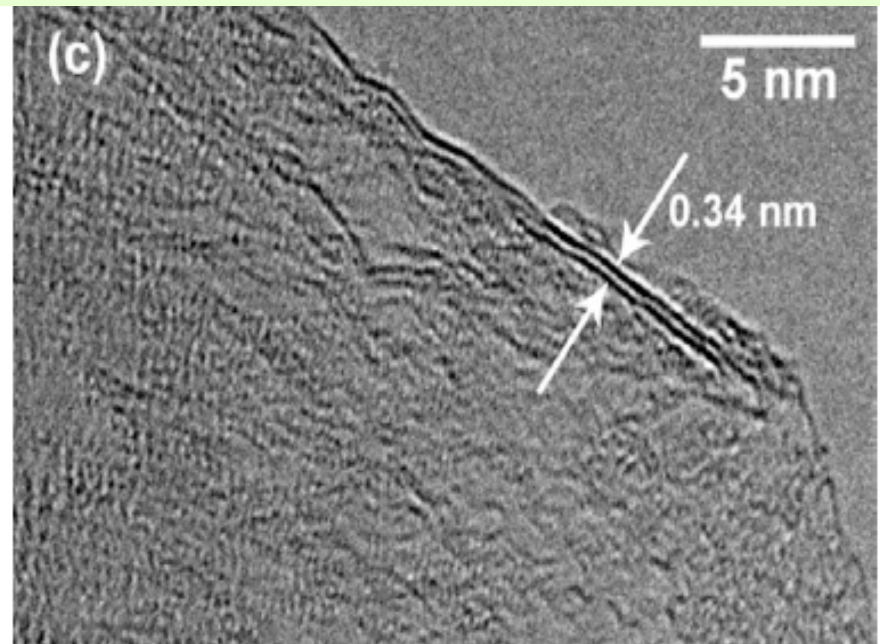
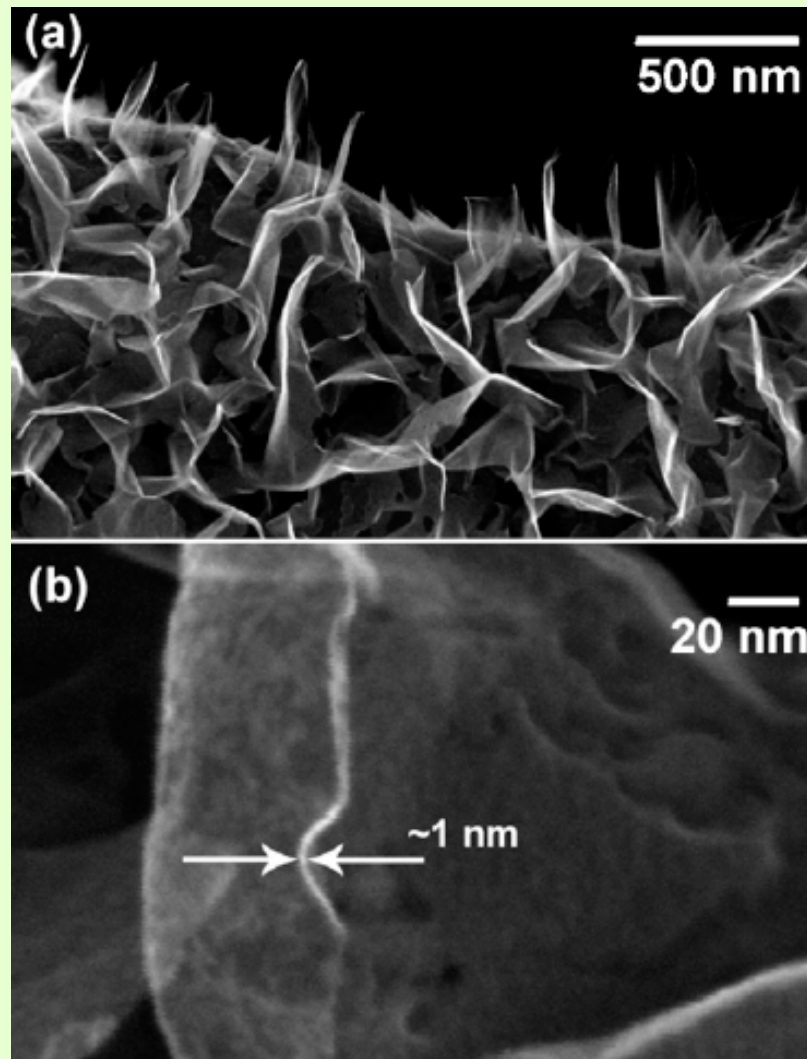
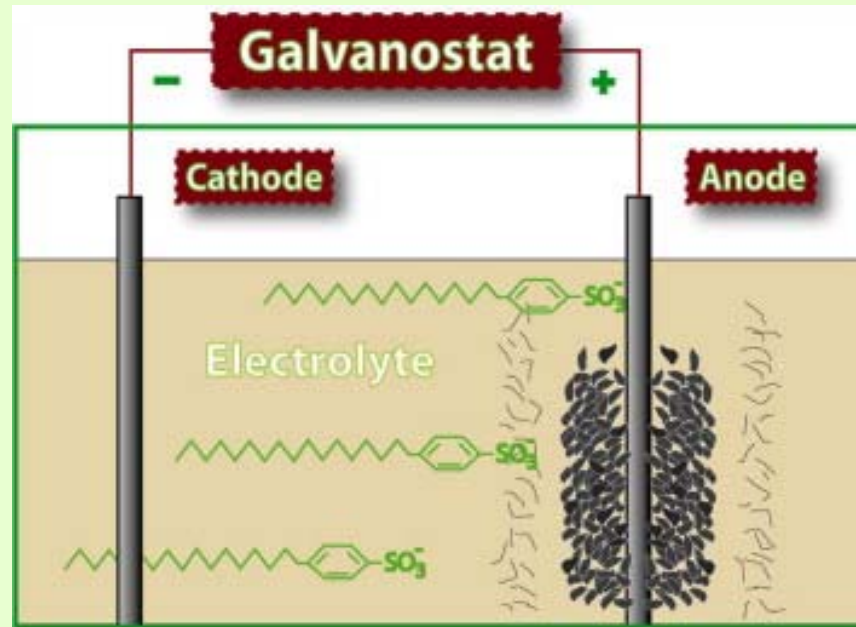


Fig. 3. (a) SEM image of typical nanosheets deposited on a Ni grid in order to show both plan and cross-section views in the same image. The nanosheets have a smooth surface morphology and are free-standing perpendicular to the substrate surface. (b) High magnification SEM image of one nanosheet edge with a thickness of ~ 1 nm. (c) HRTEM image of a single nanosheet; two parallel fringes at the fold-back location on the edge show that the sheet consists of only two graphene layers, and the distance between the two fringes is 0.34 nm.

Electrochemical Preparation of Graphene



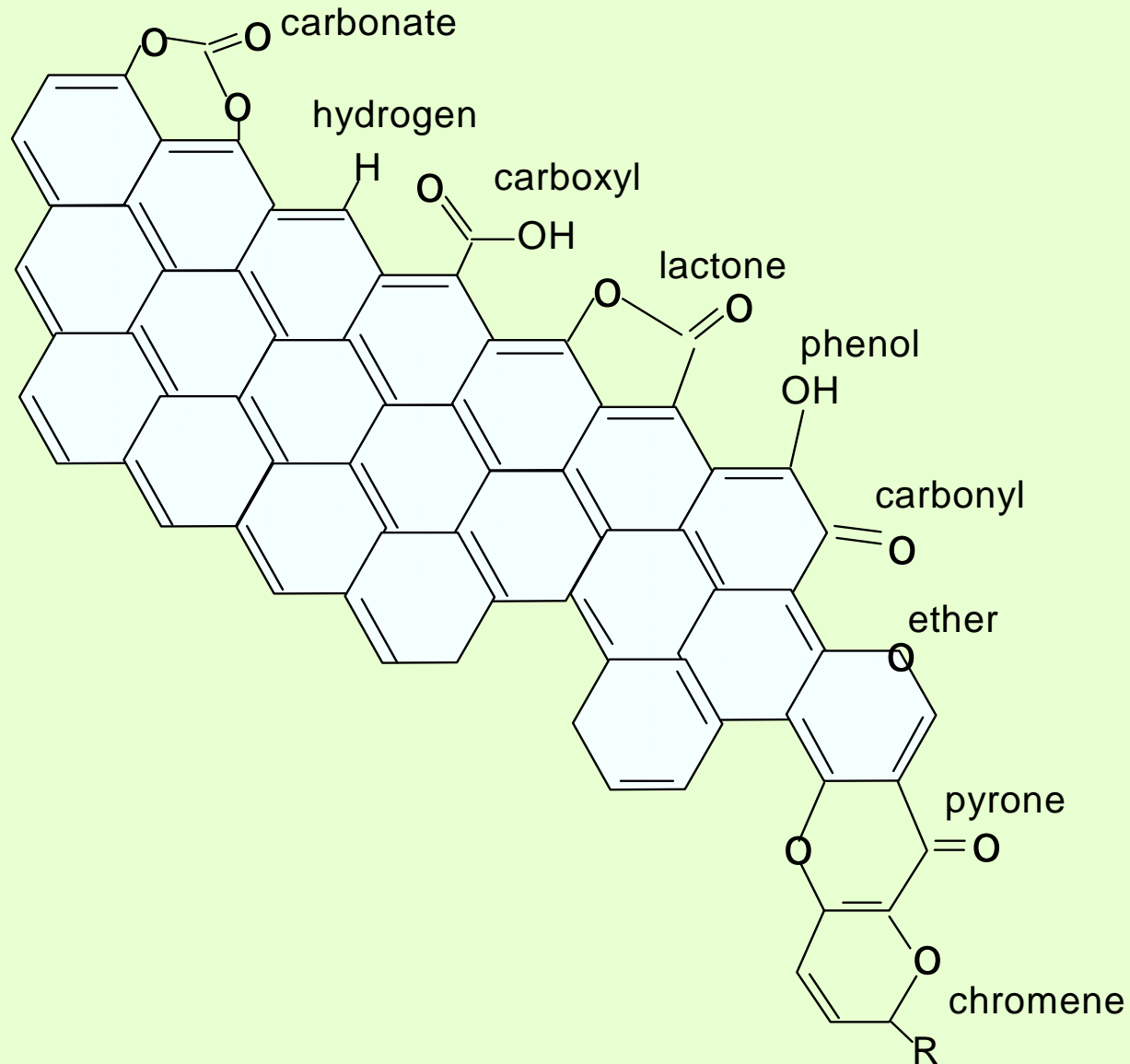
Electrolytic exfoliation

Valles, C.; et al *J Am Chem Soc* **2008**, *130*, (47), 15802-15804.

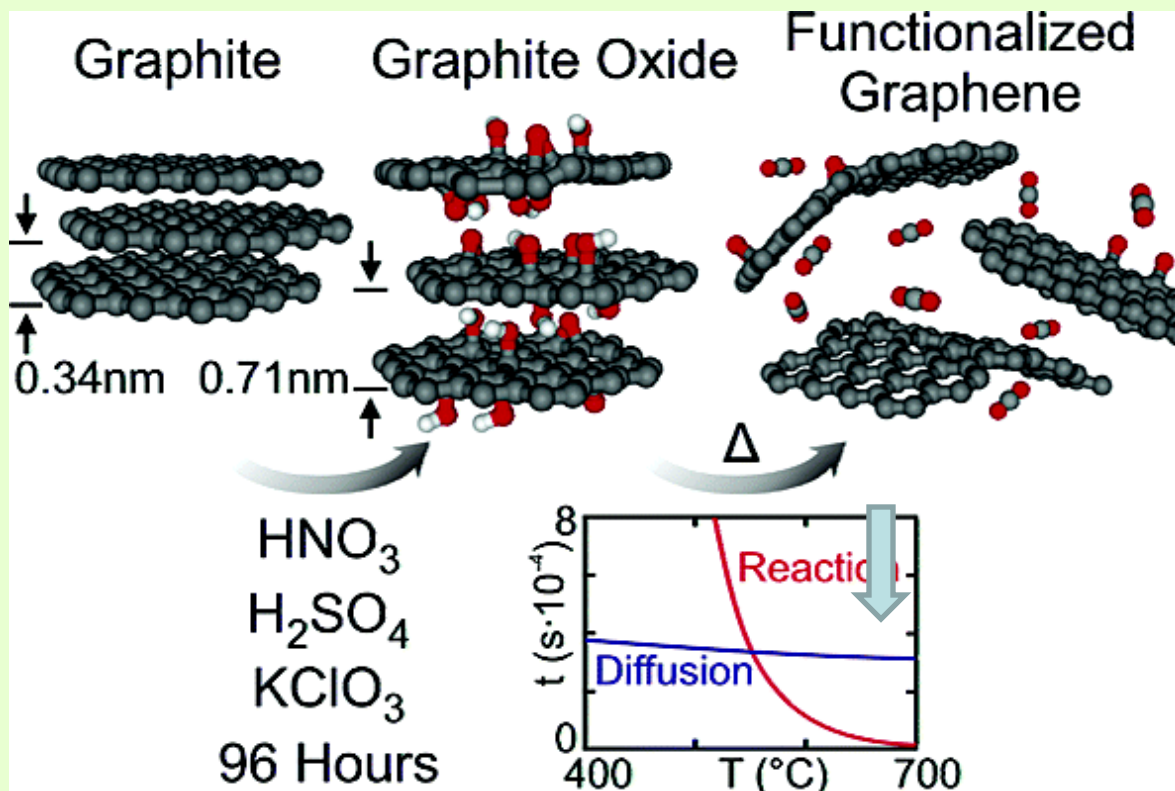
Tung, V. C.; et al *Nat Nano* **2009**, *4*, (1), 25-29.

Wang, G.; et al *Carbon* **2009**, *47*, 3242-3246.

NGP Functional groups



Preparation of Functionalized Graphene



Hummers–Offeman methods

Jang, B.; Zhamu, A. *J. Mater. Sci.* **2008**, *43*, 5092-5101

McAllister M. J., et al. *Chem. Mater.* **2007**; *19*(18):4396-4404.

Features and Properties

- Ultra-high Young's modulus (1,000 GPa) and **highest intrinsic strength (~ 130 GPa)**.
- Exceptional in-plane electrical conductivity (up to ~ 20,000 S/cm).
- **Highest thermal conductivity (up to ~ 5,300 W/(m \times K)).**
- High specific surface area (up to ~ 2,675 m²/g).
- Outstanding resistance to gas permeation.
- Readily surface-functionalizable.
- Dispersible in many polymers and solvents.
- High loading in nanocomposites.

Features and Properties:

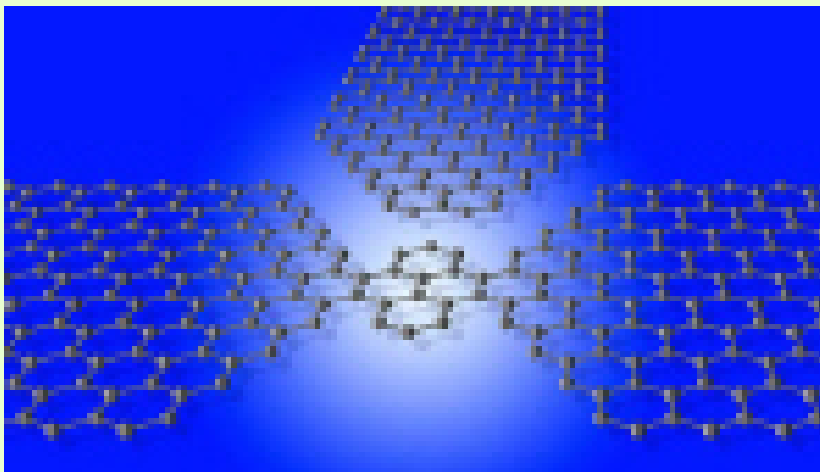
(a) Electronic/Magnetic/Optic

- Electrons in a single-layer NGP behave like massless relativistic particles, travel at speeds of around 10^6 m/s .
- The dimensions (**width and thickness**) of a graphene sheet are “**intrinsic**” material characteristics.

Atomically Thin Carbon Films

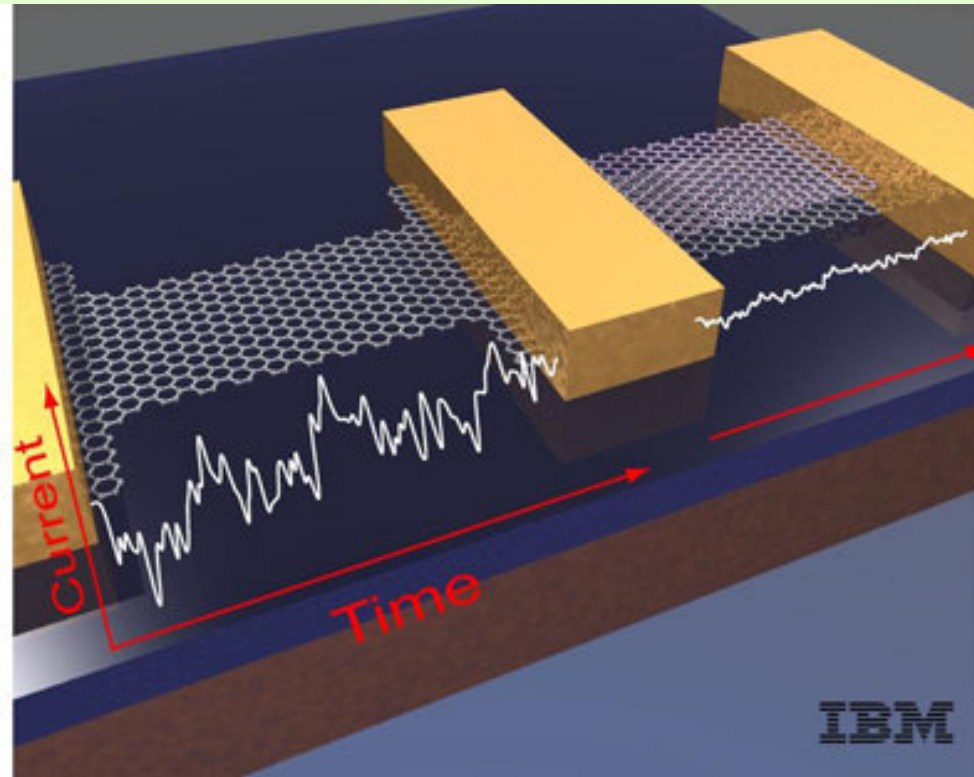
- Mono-crystalline graphitic films, **a few atoms thick**, are **metallic**.
 - Two-dimensional semimetal with a tiny overlap between valence and conductance bands.
- Exhibit a strong ambipolar electric field effect such that **electrons and holes in concentrations up to $10^{13}/\text{cm}^2$** can be induced by applying gate voltage.
- The intrinsic mobility of graphene was around **$200,000 \text{ cm}^2/\text{Vs}$** . **This value is more than 100 times higher than that of silicon** and over 20 times higher than gallium arsenide (1500 and 8500 cm^2/Vs , respectively).

- Single-layer graphene is a “zero-gap” semiconductor.
- One way of creating energy gaps is to make it into an extremely thin wire so that its electrons are confined to move in only one dimension, creating a series of electron energy levels separated by gaps.
- Novoselov, et al. use a combination of electron beam lithography and reactive plasma etching to carve small islands out of large graphene sheets to quantum-confine electrons.



Graphene: Frequency Multiplier

- Sergey Mikhailov, Univ. of Augsburg, predicts that when graphene is irradiated by EM waves, it **emits radiation at higher frequency harmonics and can thus work as a frequency multiplier.**
- It has been difficult to produce frequencies higher than 100GHz and up to 1–10THz (10^{12} Hz, the so-called terahertz gap).
- **Terahertz radiation penetrates many materials (except metals):**
 - can be used to "see" through packages at airports, for example."
 - could be used to image cancer tumours for early disease diagnosis"



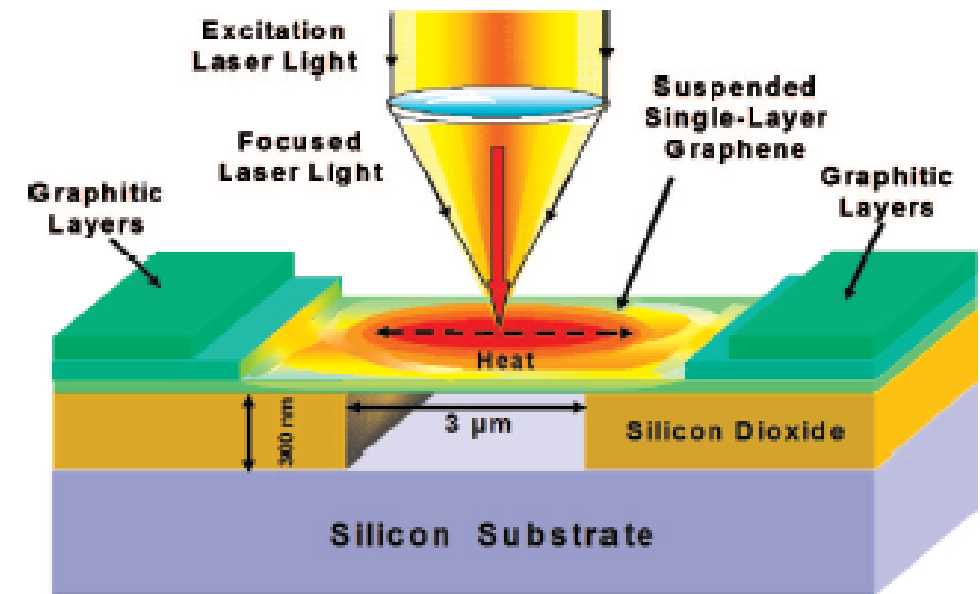
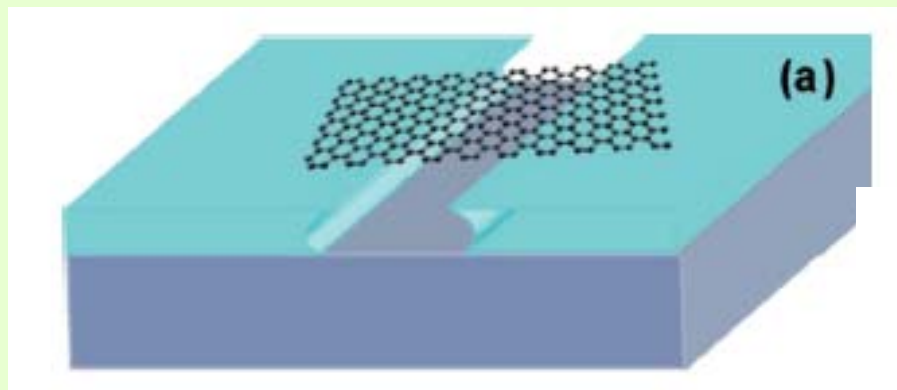
Graphene transistor switches on and off at 100 billion times per second. The 100-gigahertz speed is about 10 times faster than any silicon equiv

Features and Properties:

(b) Thermal

Highest thermal conductivity, $\sim 5,300 \text{ W/(m-K)}$!!

(A. Balandin, et al. "Superior Thermal Conductivity of Single-Layer Graphene," *Nano Lett.*, 8 (3), 902–907, 2008.)



Features and Properties: (c) Mechanical

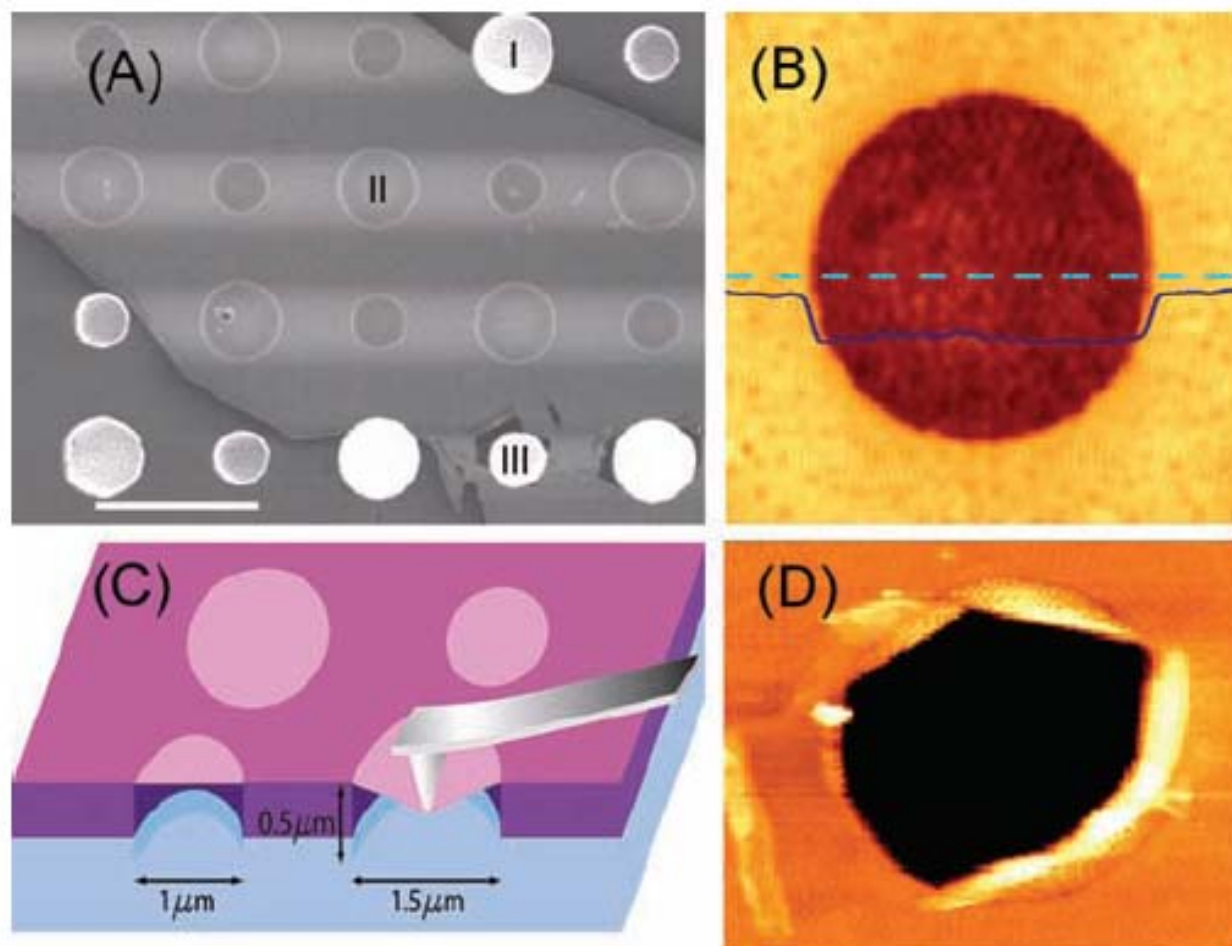
Estimated physical constants of CNTs, CNFs, and NGPs.

| Property | Single-Walled CNTs | Carbon Nano- Fibers | NGPs |
|------------------|------------------------------|---|-------------------------------|
| Specific gravity | 0.8 g/cm ³ | 1.8 (AG) -2.1 (HT) g/cm ³ AG = as grown; HT = heat- treated (graphitic) | 2.2 g/cm ³ |
| Elastic modulus | ~ 1 TPa (axial direction) | 0.4 (AG)-0.6 (HT) TPa | ~ 1 TPa (in- plane) |
| Strength | 50-100 GPa | 2.7 (AG)-7.0 (HT) GPa | ~ 130 GPa |

Intrinsic strength

C. Lee, et al, Science, 321 (July 2008) 385.

Fig. 1. Images of suspended graphene membranes. **(A)** Scanning electron micrograph of a large graphene flake spanning an array of circular holes 1 μm and 1.5 μm in diameter. Area I shows a hole partially covered by graphene, area II is fully covered, and area III is fractured from indentation. Scale bar, 3 μm . **(B)** Noncontact mode AFM image of one membrane, 1.5 μm in diameter. The solid blue line is a height profile along the dashed line. The step height at the edge of the membrane is about 2.5 nm. **(C)** Schematic of nanoindentation on suspended graphene membrane. **(D)** AFM image of a fractured membrane.



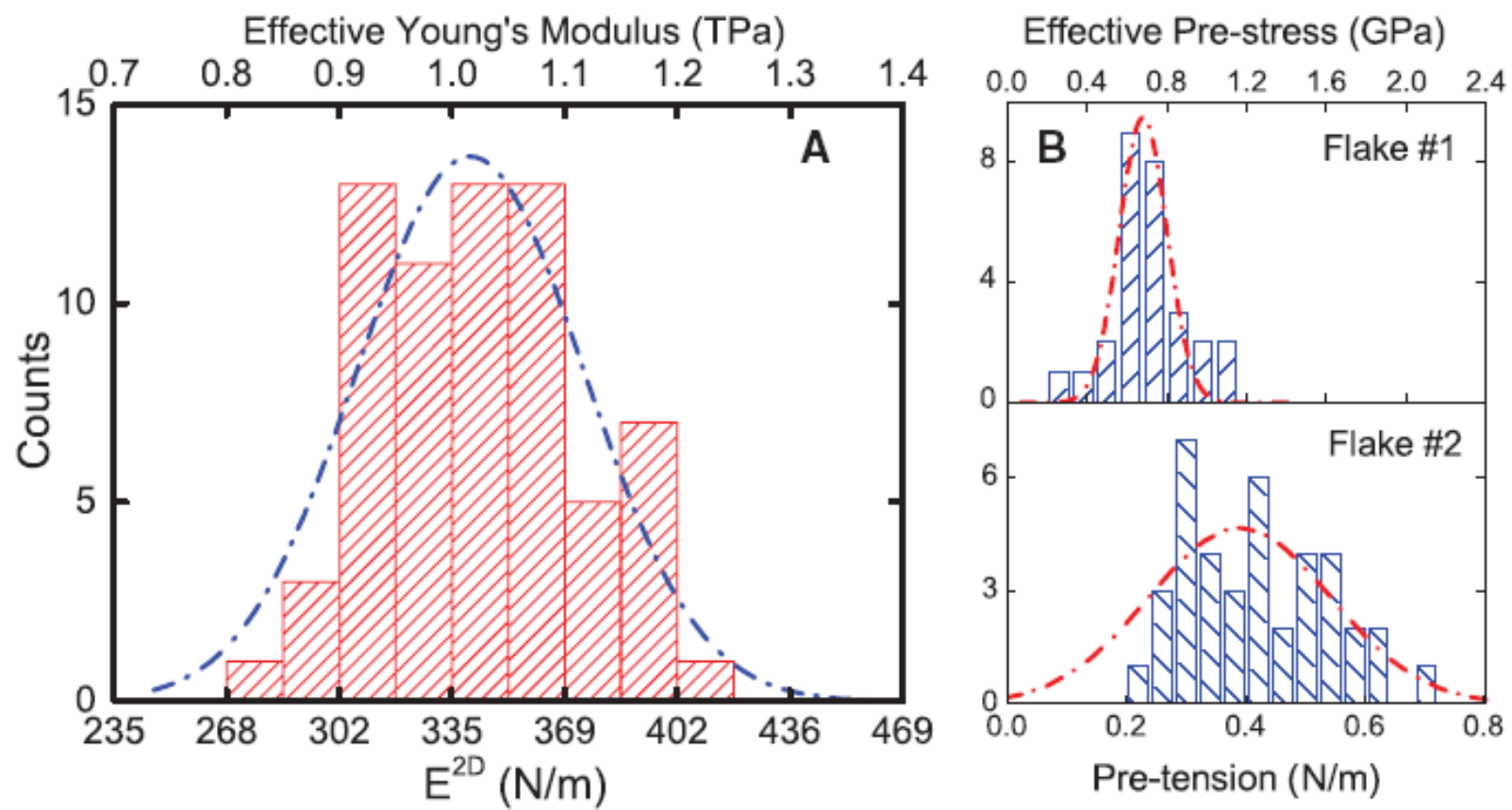


Fig. 3. Elastic response test results. **(A)** Histogram of elastic stiffness. **(B)** Histogram of film pretensions. Dashed lines in both plots represent Gaussian fits to data. The effective Young's modulus and prestress were obtained by dividing by the graphite interlayer spacing.

Intrinsic strength = 130 GPa !!

$E = 1 \text{ TPa} = 1,000 \text{ GPa}$

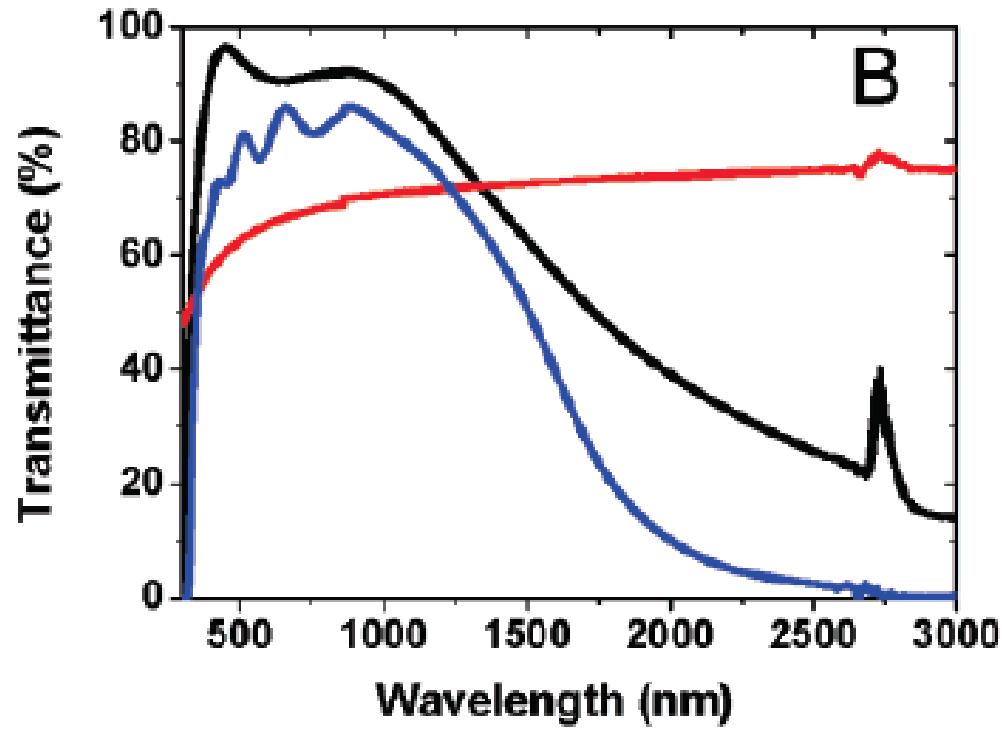


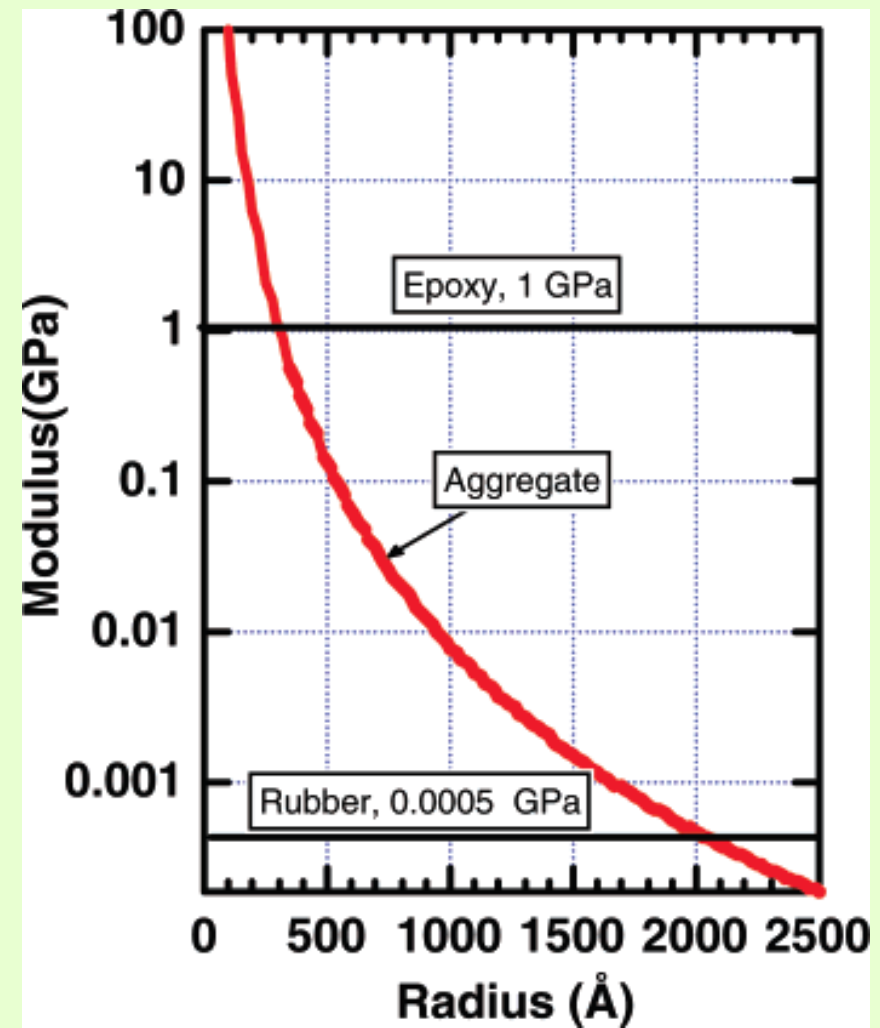
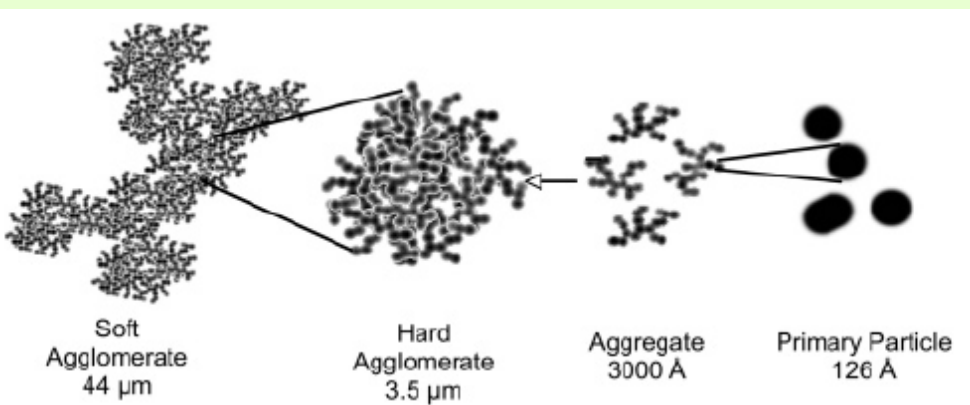
Figure 2. Structure and transmittance of graphene films. (A) HRTEM image of graphene films with corresponding SAED pattern (inset). (B) Transmittance of a ca. 10 nm thick graphene film (red), in comparison with that of ITO (black) and FTO (blue).

NGP Nanocomposites?

Parameters to consider:

- Graphene platelet **thickness** (number of graphene planes): strength, modulus, and thermal conductivity.
- **Length-to-thickness ratio**: percolation threshold for electrical conductivity
- Platelet **orientation**: all properties
- **Functionality**: interfacial bonds

Reinforcement Effect of Nano-filters in Polymer; (A) Elastic modulus



Schaefer, D. W.; et al. *Macromolecules* 2007, 40(24), 8501-8517

Reinforcement Effect of Nano-filters in a Matrix Material; (B) Strength

Griffith eq.: $\sigma_f = (E\chi/\pi c)^{1/2}$

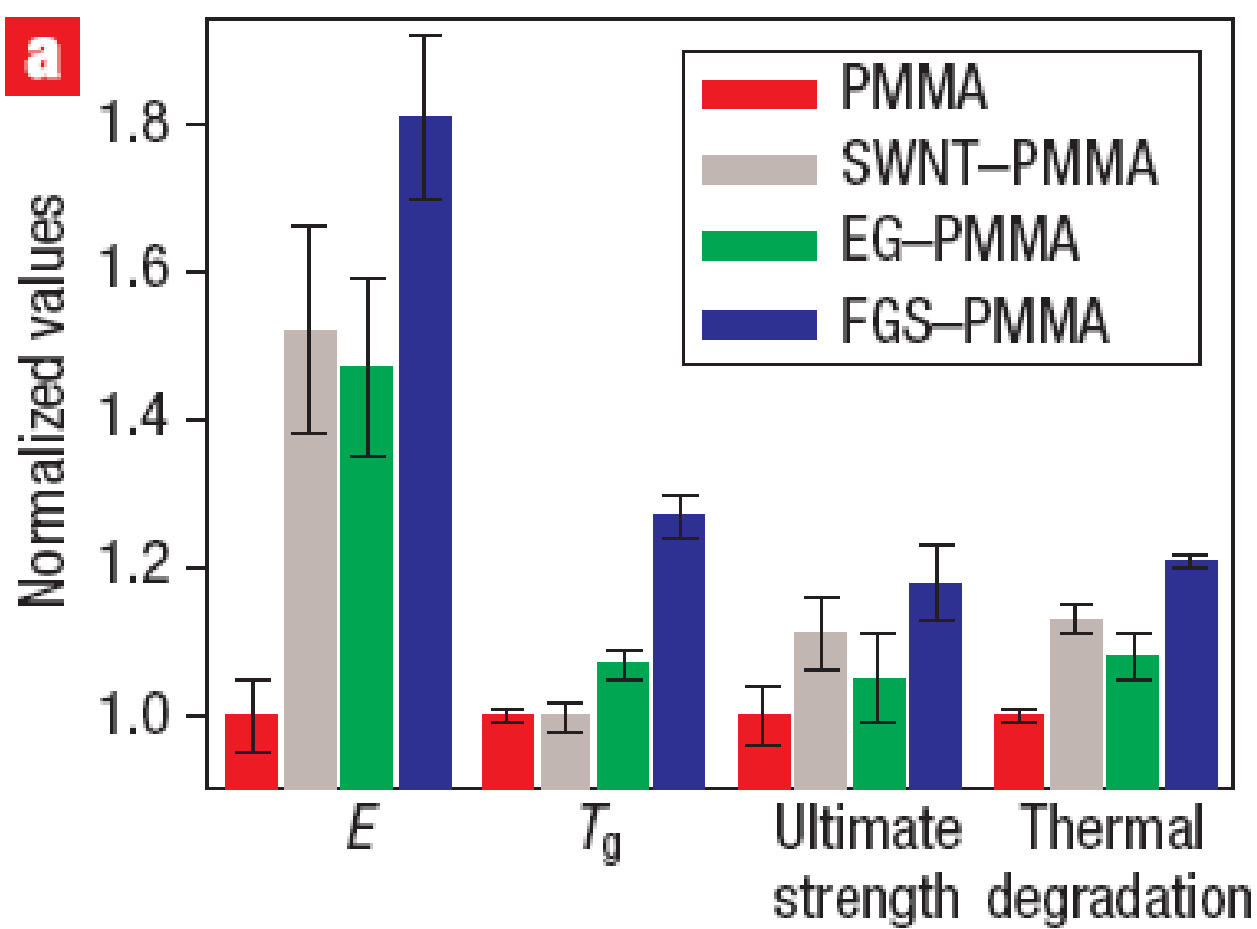
σ_f = strength;

E = modulus,

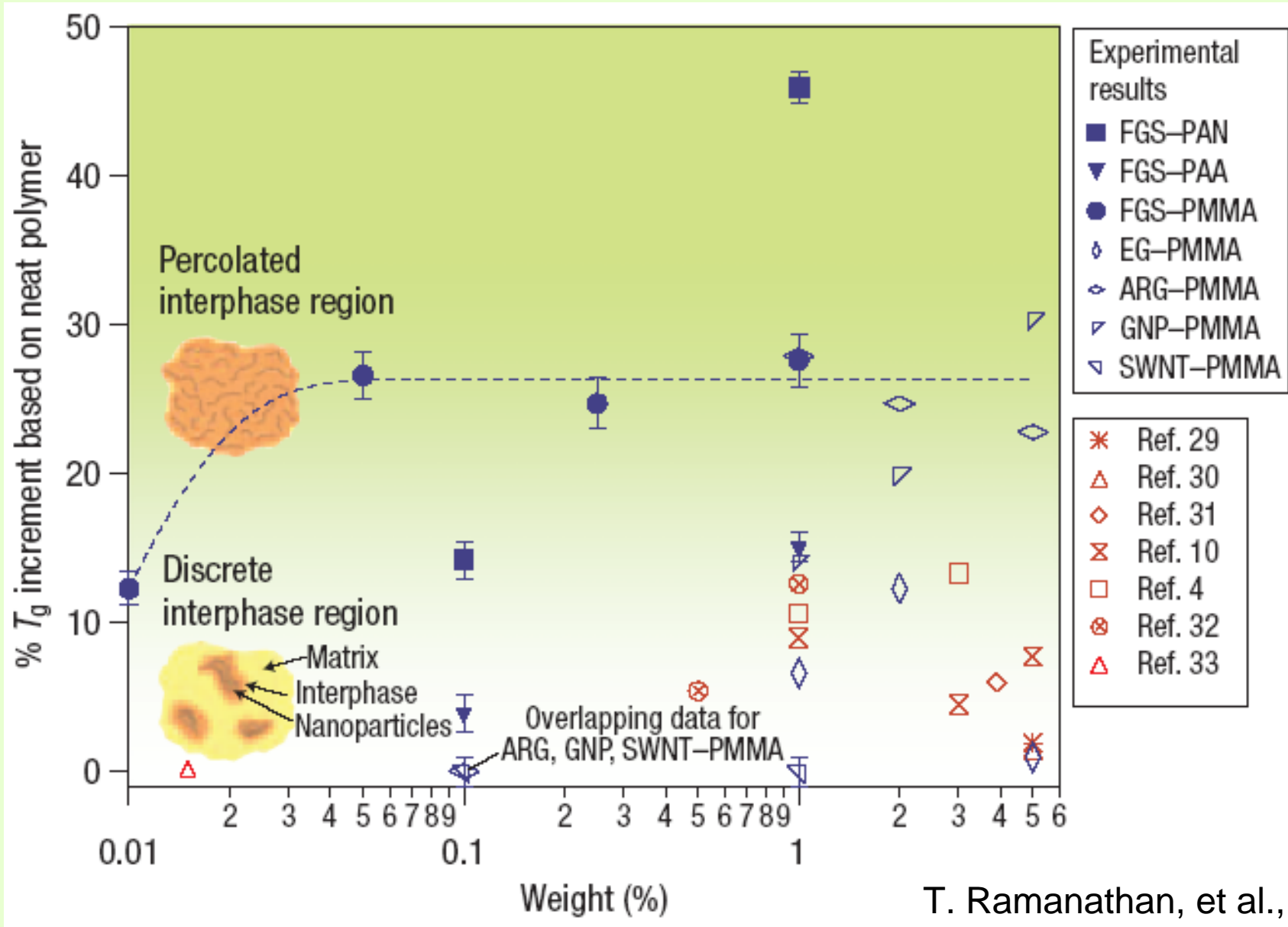
χ = surface free energy;

C = crack size

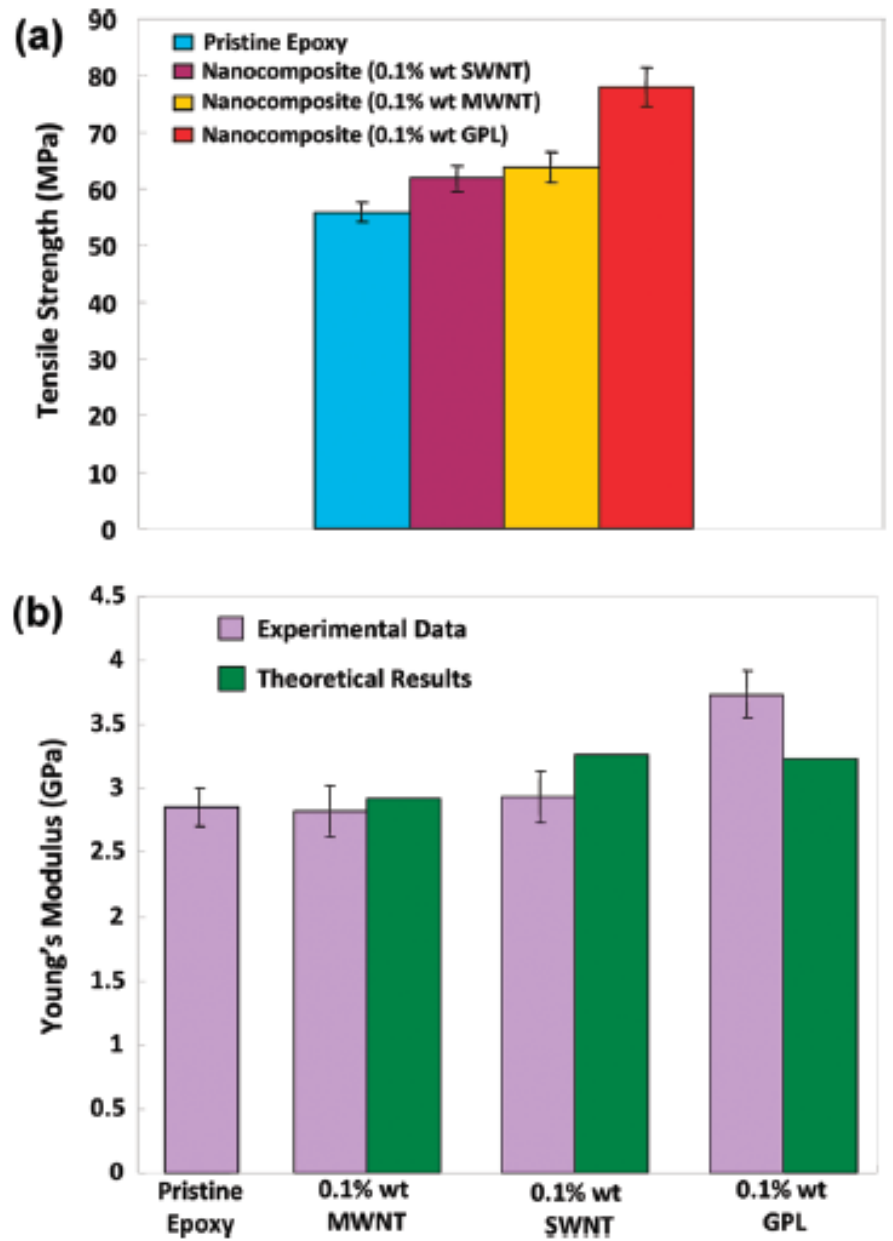
NGP Nanocomposites



Thermomechanical property improvements for 1 wt% FGS-PMMA compared to SWNT-PMMA and EG-PMMA composites. Neat PMMA values are E (Young's modulus) ~2.1 GPa, T_g ~105 °C, ultimate strength ~ 70 MPa, thermal degradation temperature ~285°C; T. Ramanathan, et al., *Nature Nanotechnology*, May 2008.



T. Ramanathan, et al.,



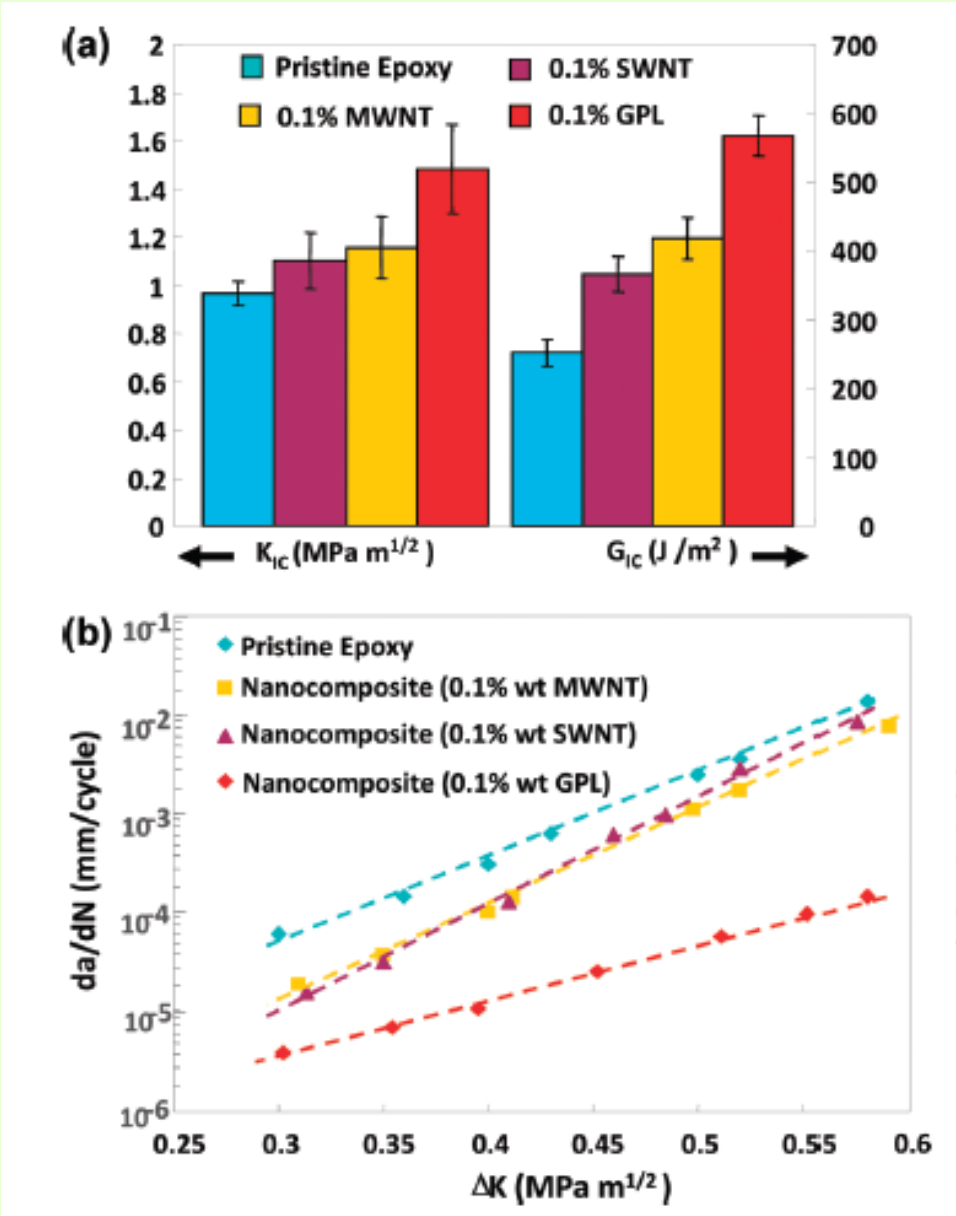


Figure 4. Fracture and fatigue testing. (a) Mode I fracture toughness (K_{Ic}) and fracture energy (G_{Ic}) for the baseline epoxy and GPL/epoxy, MWNT/epoxy, and SWNT/epoxy nanocomposites at ~ 0.1 wt % fraction of nanofillers. (b) Fatigue crack propagation testing; crack growth rate (da/dN) plotted as a function of the stress intensity factor amplitude (ΔK) for the pristine epoxy and nanocomposite samples with ~ 0.1 wt % of GPL, ~ 0.1 wt % of SWNT, and ~ 0.1 wt % of MWNT additives. The error in estimation of weight fraction for the various nanocomposite samples is estimated to be less than $\pm 0.002\%$.

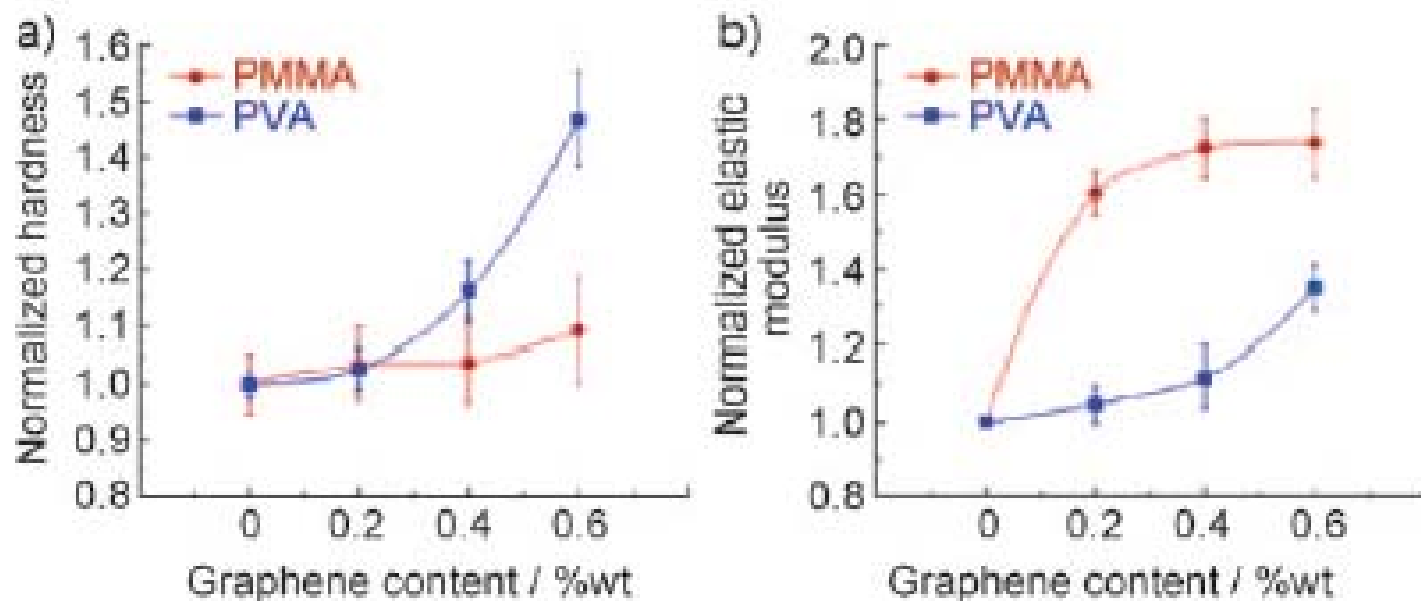


Figure 43. Normalized a) hardness (H) and b) elastic modulus (E) plotted as a function of graphene content for PVA and PMMA composites. (The pristine values of PMMA and PVA are $E_{\text{PMMA}} = 2.1 \text{ GPa}$, $H_{\text{PMMA}} = 140 \text{ MPa}$, $E_{\text{PVA}} = 0.65 \text{ GPa}$, and $H_{\text{PVA}} = 38 \text{ MPa}$). (From Ref. [187].)

B. Das, K. E. Prasad, U. Ramamurty, C. N. R. Rao, *Nanotechnology* **2009**, *20*, 125705.

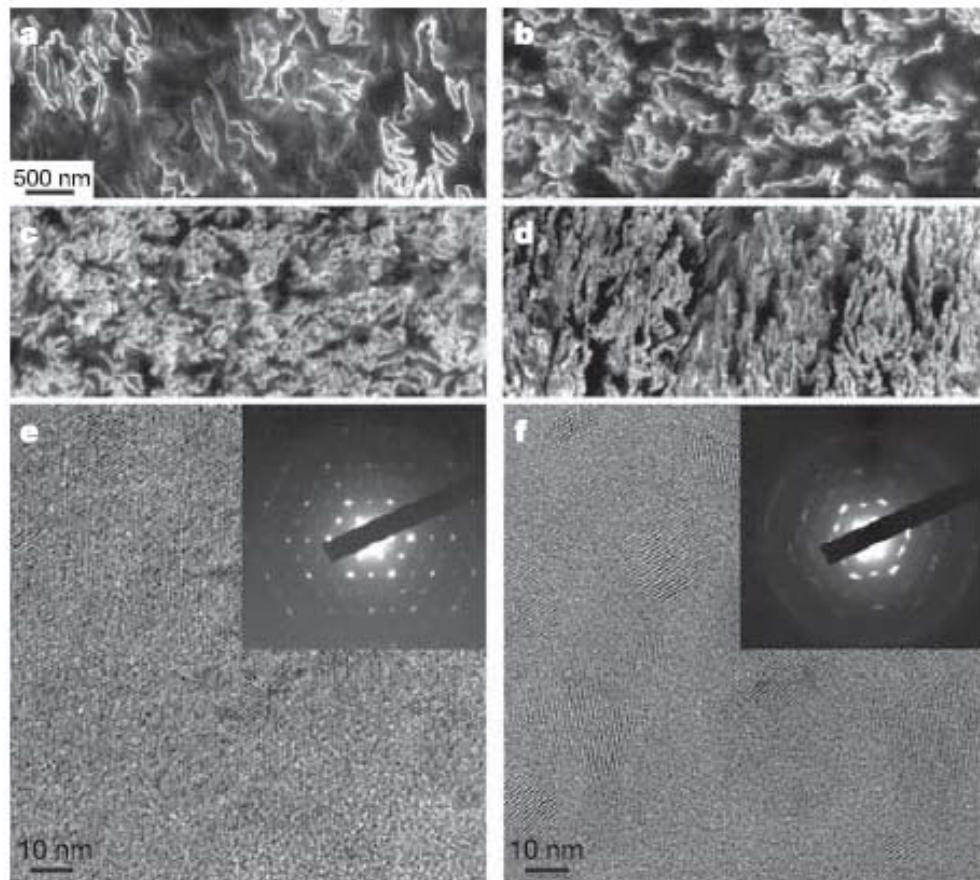


Figure 2 | SEM and TEM images of graphene-polystyrene composite.
a–d, SEM images of the microtomed composites reveal different morphologies of the graphene sheets, including their packing, at different concentrations (vol.%): a, 0.24; b, 0.96; c, 1.44; and d, 2.4. Scale bar, shown in a, applies to a–d. e, f, High-resolution phase contrast images and SAED patterns (inset) of e, cast film made from powder composite, and f, microtomed composite sample. The SAED patterns show the six-fold rotational symmetry expected for diffraction with the beam incident along [0001]. Our experimentally obtained patterns show all of the reflections expected for such single graphene-based sheets. The d spacings associated with the spots were determined using both gold and graphite calibrants, and the first five sets of spots correspond to d -spacings (\AA) of 4.23, 2.45, 2.12, 1.42 and 1.23. More details are presented in Supplementary Information.

S. Stankovich, et al. *Nature*,
442 (July 2006) 282.

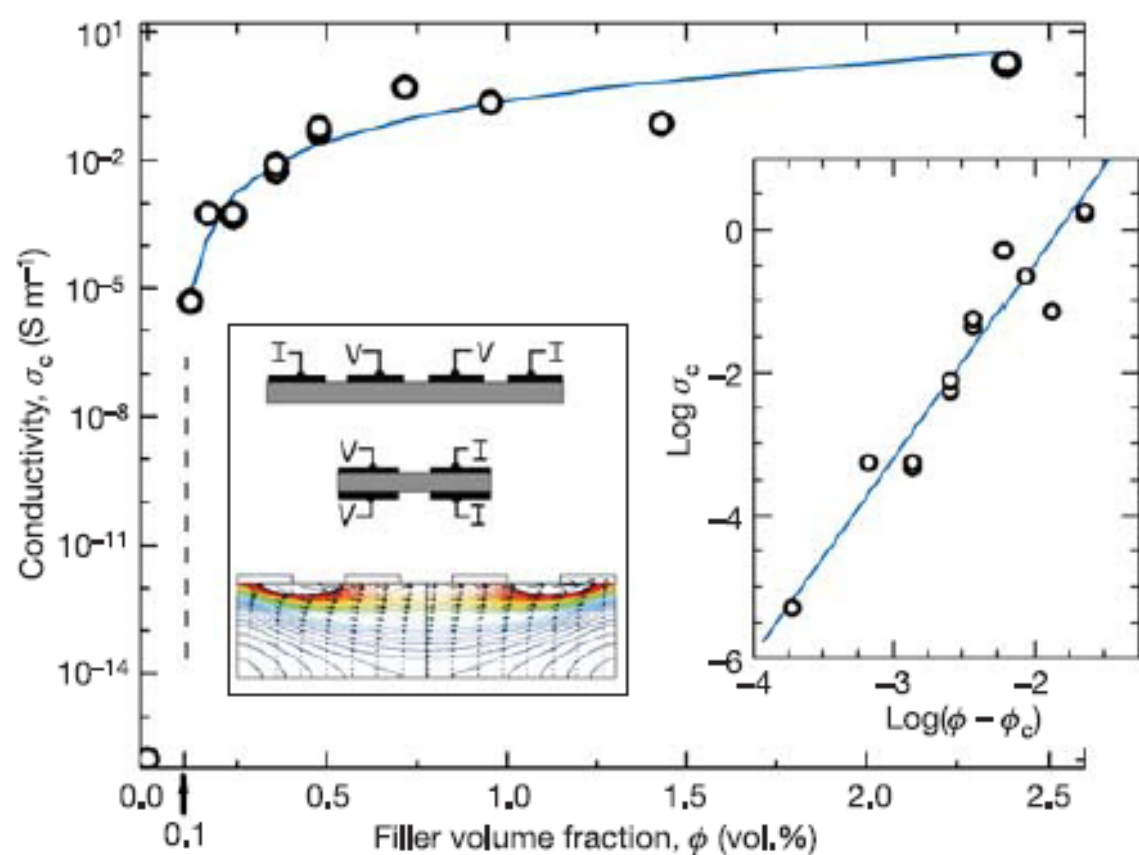


Figure 3 | Electrical conductivity of the polystyrene-graphene composites as a function of filler volume fraction. Main figure, composite conductivity, σ_c , plotted against filler volume fraction, ϕ . Right inset, $\log\sigma_c$ plotted against $\log(\phi - \phi_c)$, where ϕ_c is the percolation threshold (see text). Solid lines in both graphs are calculated conductivities based on the fitting (inset, log–log plot) of the experimental data to the effective conductivity equation described in the text. Fitted parameters are: $t = 2.74 \pm 0.20$, $\sigma_f = 10^{4.92 \pm 0.52} \text{ S m}^{-1}$ and $\phi_c = 0.1 \text{ vol.}\%$. Left inset: top and middle

S. Stankovich, et al. *Nature*, 442 (July 2006) 282.

NGPs - the enabler for nanocomposites

- Significantly lower cost-of-use than carbon nano-tubes (CNTs).
- Comparable properties to CNTs: similar electrical conductivity, **higher thermal conductivity** and **higher specific surface area**.
- High NGP loading in a matrix (> 75% by weight).
- Low inter-platelet friction promotes reduced matrix viscosity.
- NGPs reduce fiber entanglements, thus allows higher than normal CNT and CNF loadings.
- Improves processability of nanocomposites.

Example of Market Applications

- Interconnect and heat dissipation materials in microelectronic packaging (**thermal management**);
- Electrodes in batteries and **supercapacitors**, and **bipolar plates** in fuel cells;
- **Automotive**, including fuel systems, tires (heat dissipation and stiffness enhancement), mirror housings, interior parts, bumpers, fenders, and body components that require electrostatic spray painting;
- Aerospace, including aircraft braking systems, thermal management, and **lightning strike protection**;
- Environmental applications, including waste chemical/water treatments, filtration and purification;
- **EMI/RFI shielding** for telecommunications devices (e.g., mobile phones), computers, and business machines;
- Potential market size for conductive nano fillers and nanocomposites is forecast to reach **\$5-10 billion** by 2013.

NGPs for Energy Applications

- Li-ion Batteries
 - Anode active material
 - Hybrid active material
 - Electrode conductive additives
- Supercapacitor electrode
- Fuel cells
 - Bipolar plate; catalyst support
- Wind turbine blade
- Hydrogen storage material
- Solar energy
 - Transparent, conductive glass

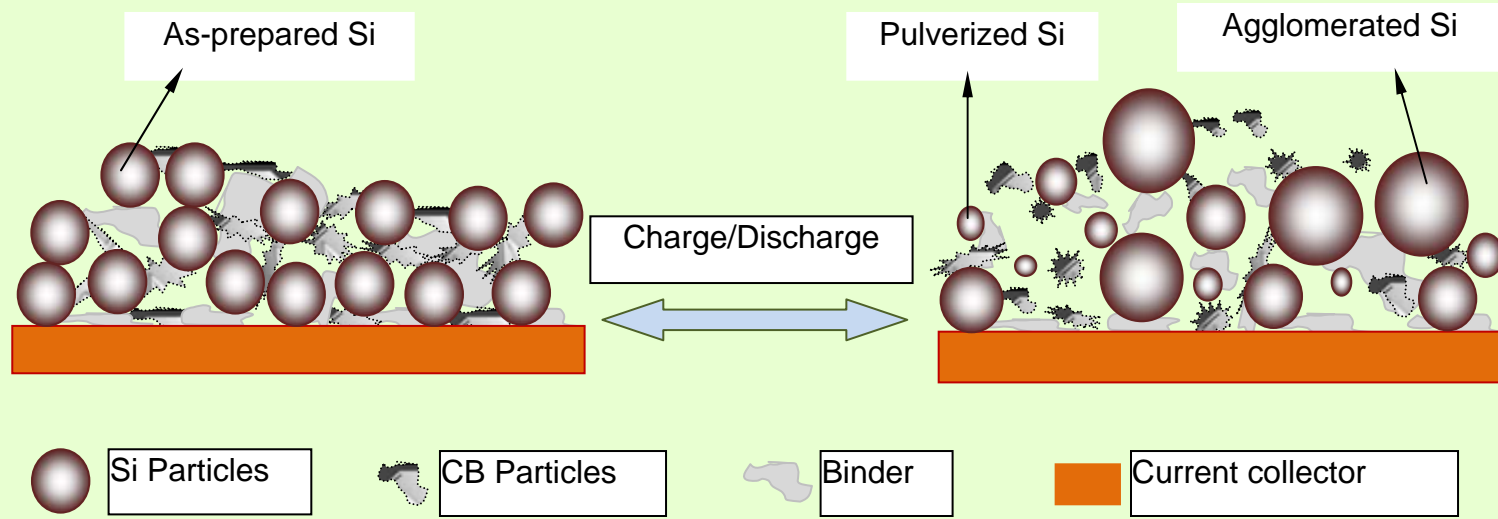


Maxwell products



Source: Internet

NGPs as a Conductive Additive

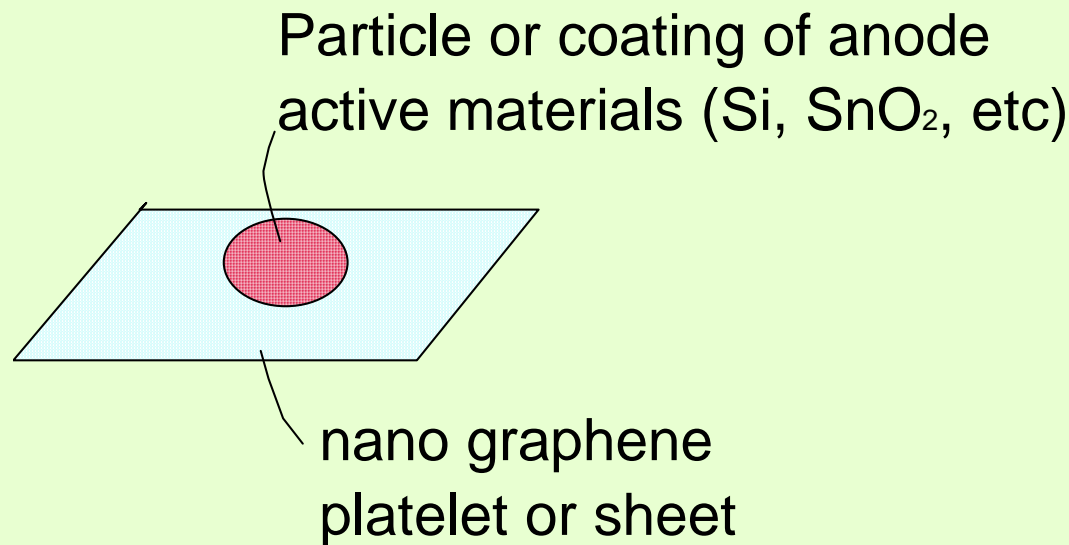


Theoretically, Si has the highest Li storage capacity (4,200 mAh/g), but undergoes a high volume expansion/shrinkage (320-380%) during charge/discharge cycles:

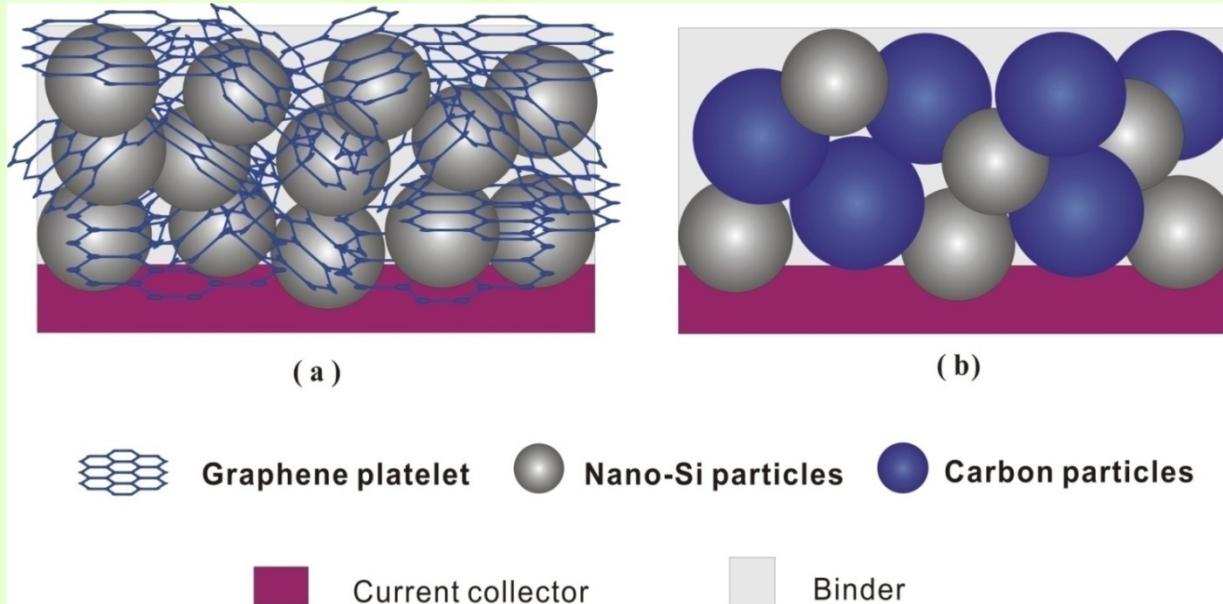
- (1) Pulverization of Si particle or thin film;
- (2) Fragmented particles lose contact with the conductive additive and current collector, resulting in significant capacity decay.

A Breakthrough Li-ion Anode Technology

- Aruna Zhamu and Bor Z. Jang, “Nano graphene platelet-based composite anode compositions for lithium ion batteries,” US Patent Appl. No. 11/982,672 (11/05/2007).
- International Patent Application: PCT/US2008/082183.

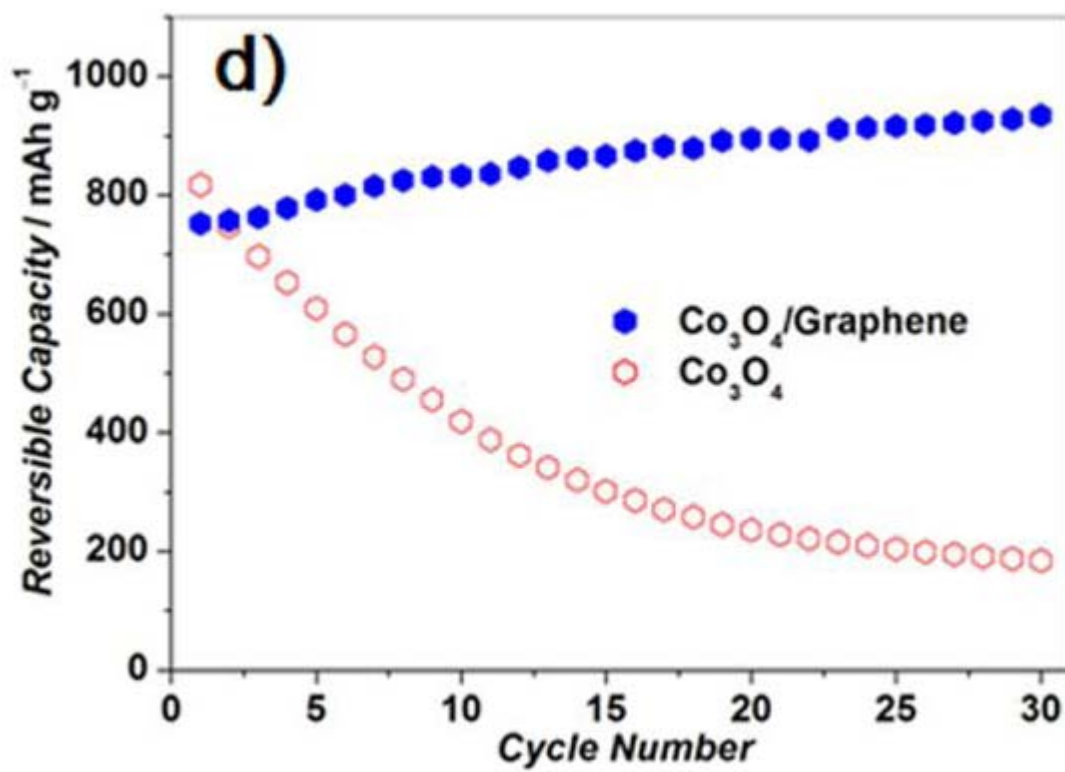
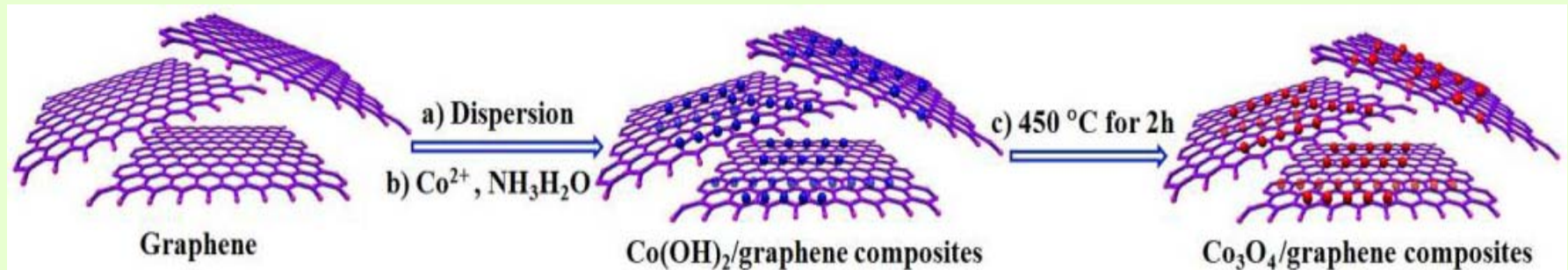


New high-capacity anode compositions: 500-2,000 mAh/g



- Increased electrode conductivity due to a percolated **graphene** network;
- Dimensional confinement of active material particles by the surrounding graphene sheets limits the volume expansion upon lithium insertion;
- SnO_2 – graphene nanocomposite form a stable 3D architecture.
- Graphene sheets prevent aggregation of nanoparticles during Li charge/discharge process.

Graphene nano sheet (GNS) + Co_3O_4 as Anode Active Materials

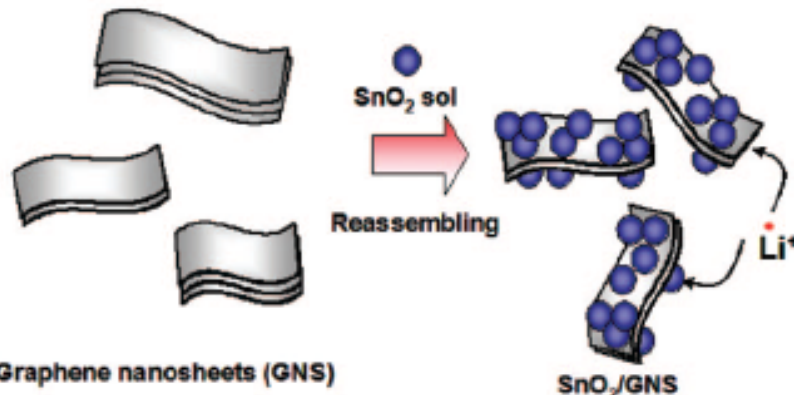


G. Wu, et al., accepted by Advanced Materials, 2010

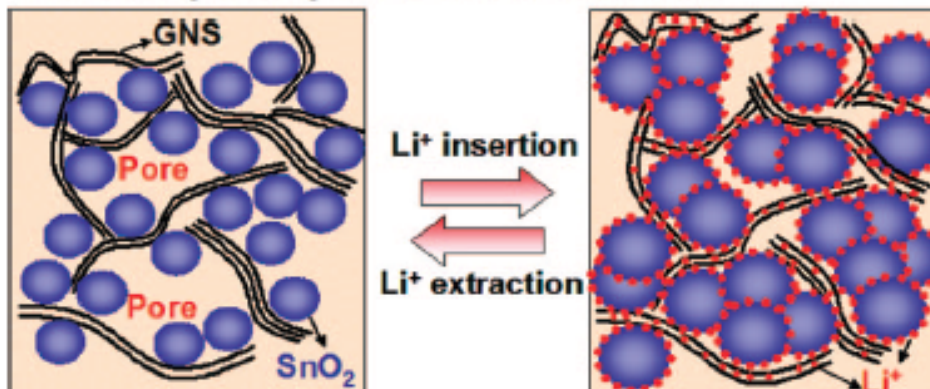
Graphene nano sheet (GNS) + SnO₂ as Anode Active Materials

Scheme 1. Schematic Illustration for the Synthesis and the Structure of SnO₂/GNS

Increased capacity: Li⁺ can be intercalated into both GNS and SnO₂



Enhanced cyclability via 3-D flexible structure



Source: S. M. Paek, et al, *Nano Letters*, 9 (2009) 72-75.

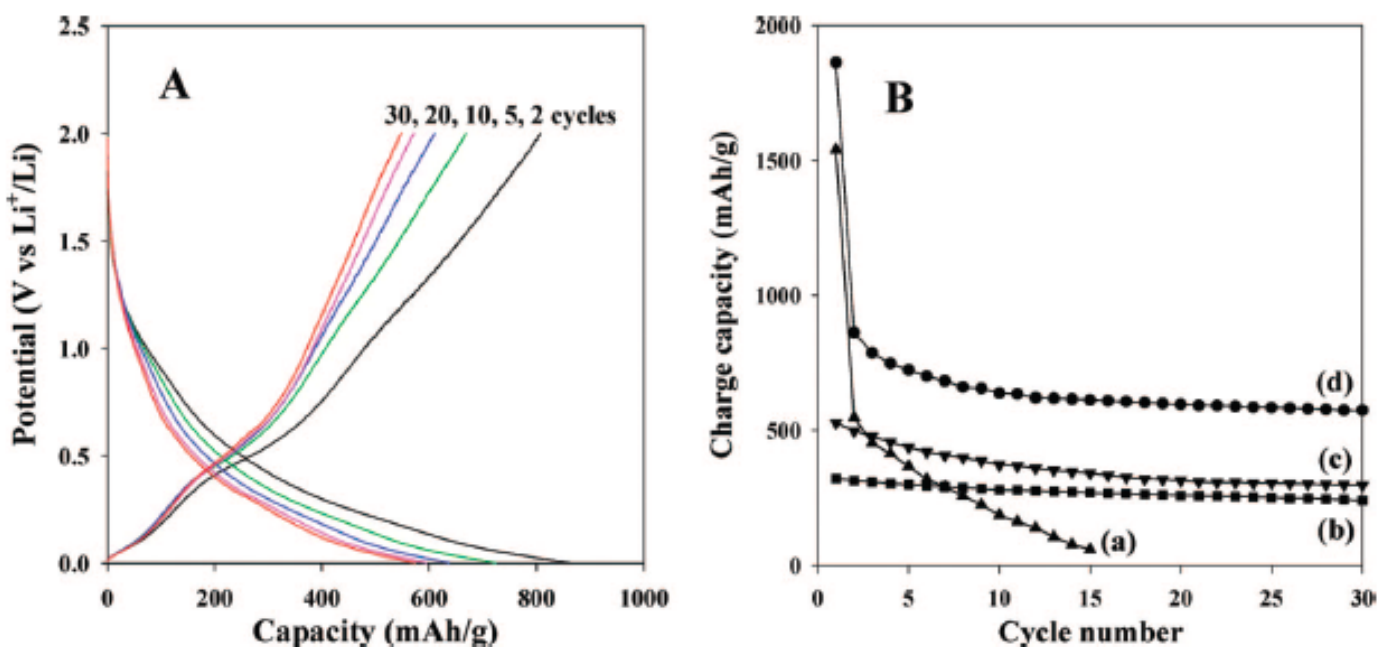
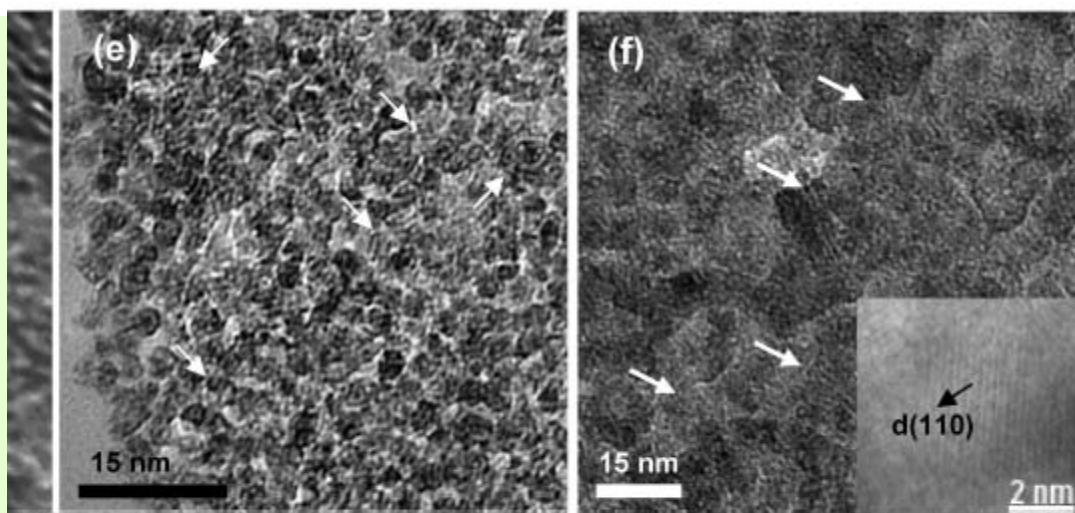


Figure 2. (A) Charge/discharge profile for SnO₂/GNS. (B) Cyclic performances for (a) bare SnO₂ nanoparticle, (b) graphite, (c) GNS, and (d) SnO₂/GNS.



GNS and SnO₂/GNS: SEM images for (a) GNS, (b) SnO₂/GNS. Cross-sectional TEM images for (e) as-prepared SnO₂/GNS, (f) heat-treated SnO₂/GNS. The white arrows denote the graphene

Graphene + SnO₂ as Anode Active Materials

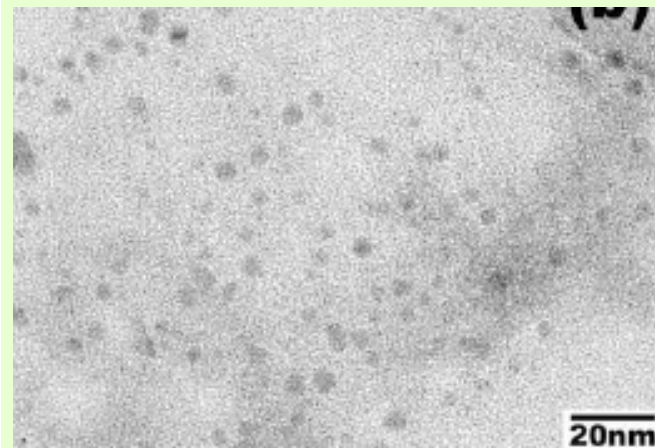
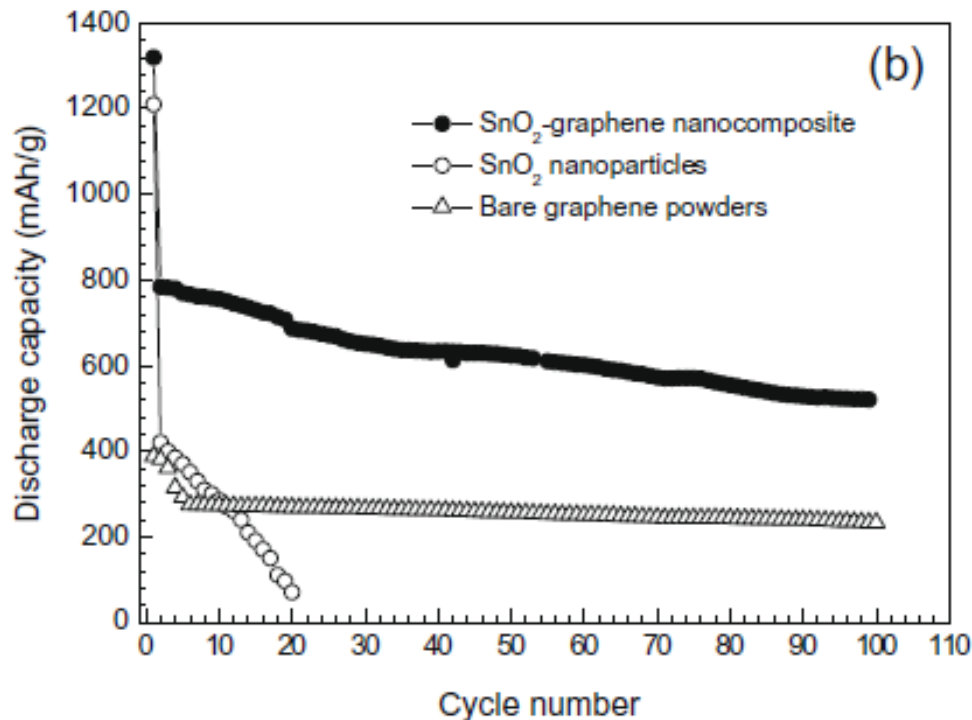
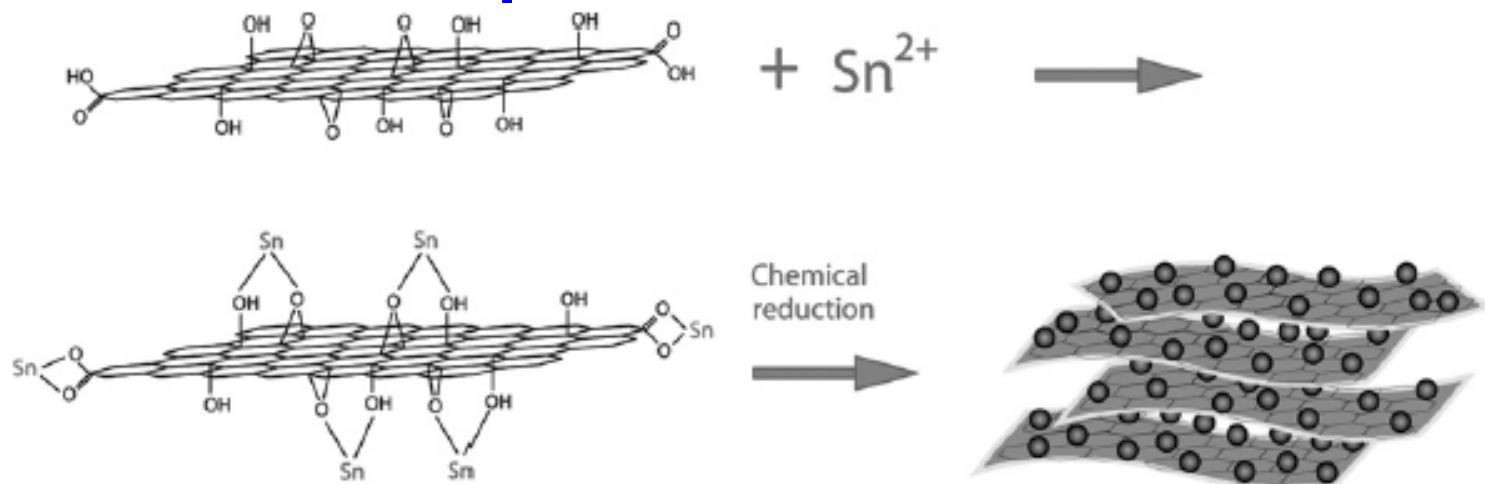


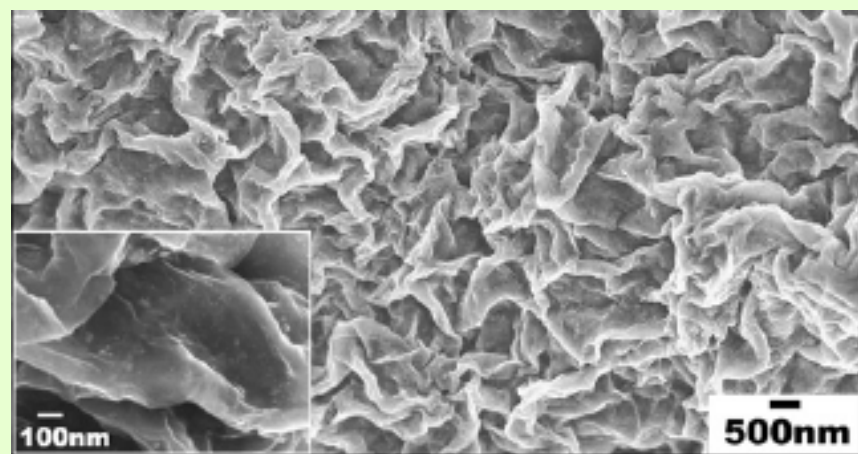
Fig. 4. (a) Charge/discharge profiles of SnO₂-graphene nanocomposite anode in a lithium ion cell. (b) Reversible lithium storage capacity vs. cycle number for SnO₂-graphene nanocomposite electrode. As a comparison, the cyclabilities of bare SnO₂ nanoparticle electrode and bare graphene electrode are also presented.

Source: J. Yao, et al, Electrochim. Communication, 11 (2009) 1849-52

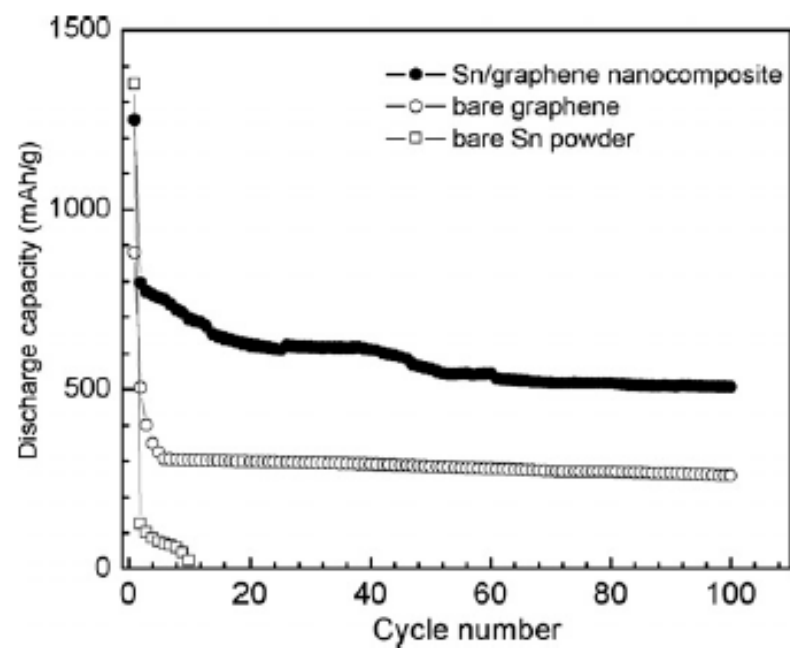
Graphene + Sn as Anode Active Materials



Scheme 1 Schematic diagram of the synthesis of the Sn/graphene nanocomposite with a 3D architecture.

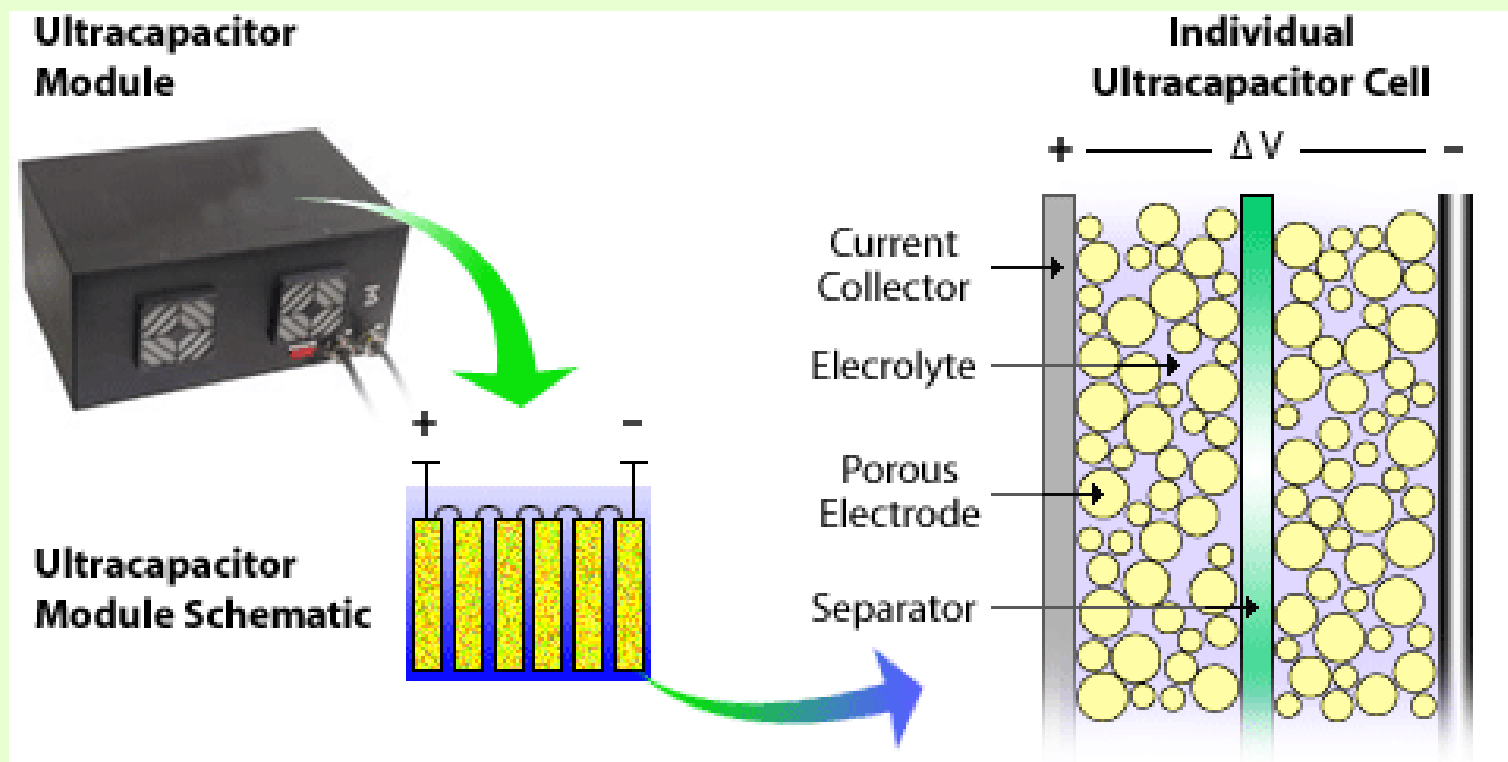


See Guoxiu Wang, Bei Wang, Xianlong Wang,
Jinsoo Park, Shixue Dou, Hyojun Ahn and
Kiwon Kim, *J. Mater. Chem.*, 2009, **19**, 8378.



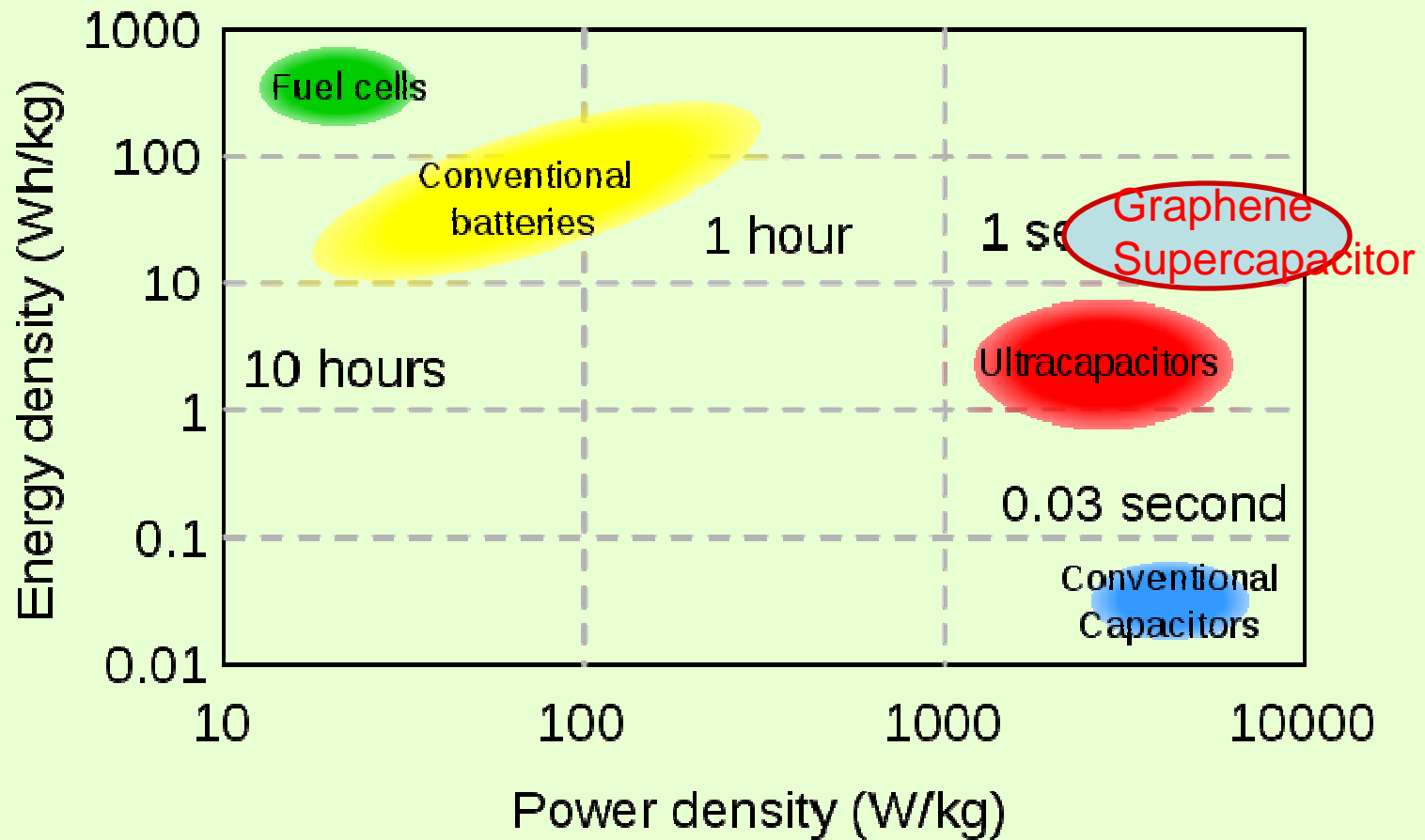
Supercapacitor

Also known as electrochemical capacitors or ultracapacitors



Activated carbon, carbon nanotube, carbon aerogel, conducting polymers, and **graphene**

(Source: UltraCapacitor.org)

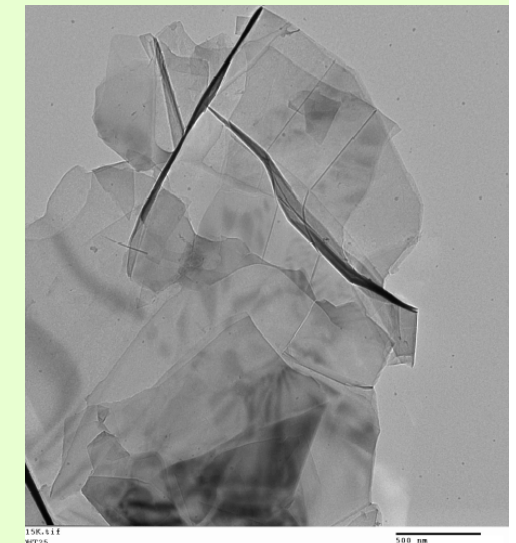
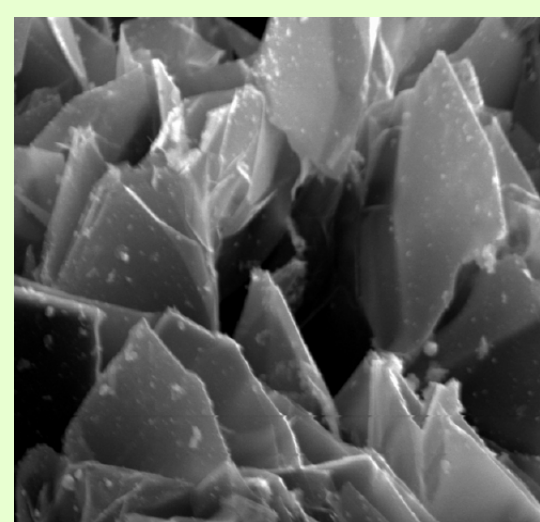


Ragone chart showing energy density vs. power density
for various energy-storage devices

(Source: UltraCapacitor.org)

Graphene

- Highest intrinsic double-layer capacitance: 21 $\mu\text{F}/\text{cm}^2$
- Ultra-high specific surface area = 2,670 m^2/g
- Ultra-high specific capacitance = 550 F/g (theoretical)
- High conductivity: low equivalent series resistance (ESR)



A Breakthrough Technology

“Nano-scaled Graphene Plate Nanocomposites for Supercapacitor Electrodes” US Pat. No. 7,623,340 (11/24/2009).

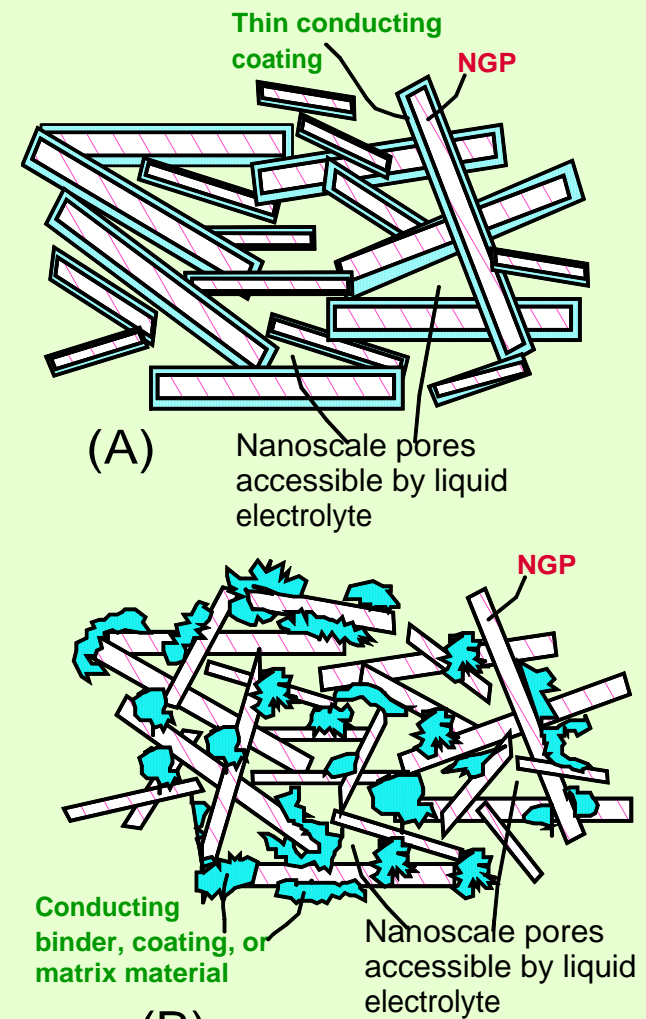
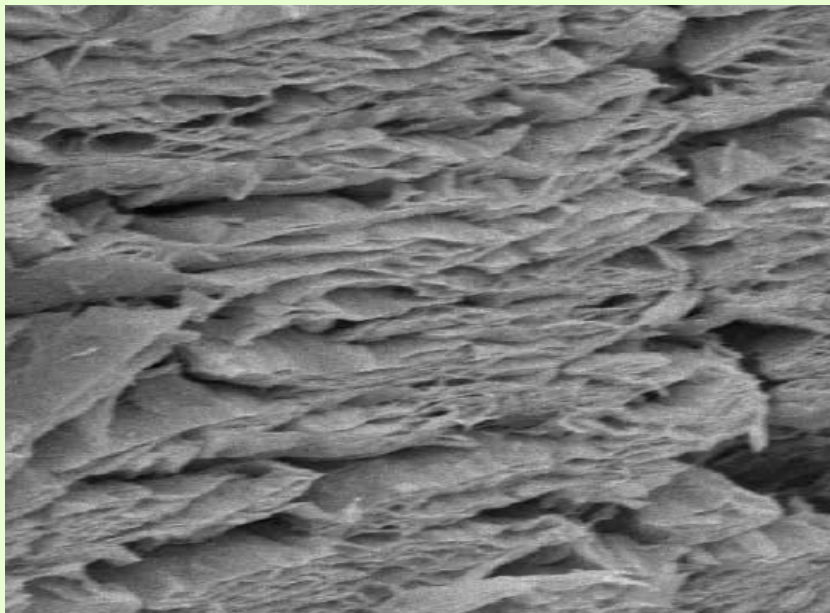
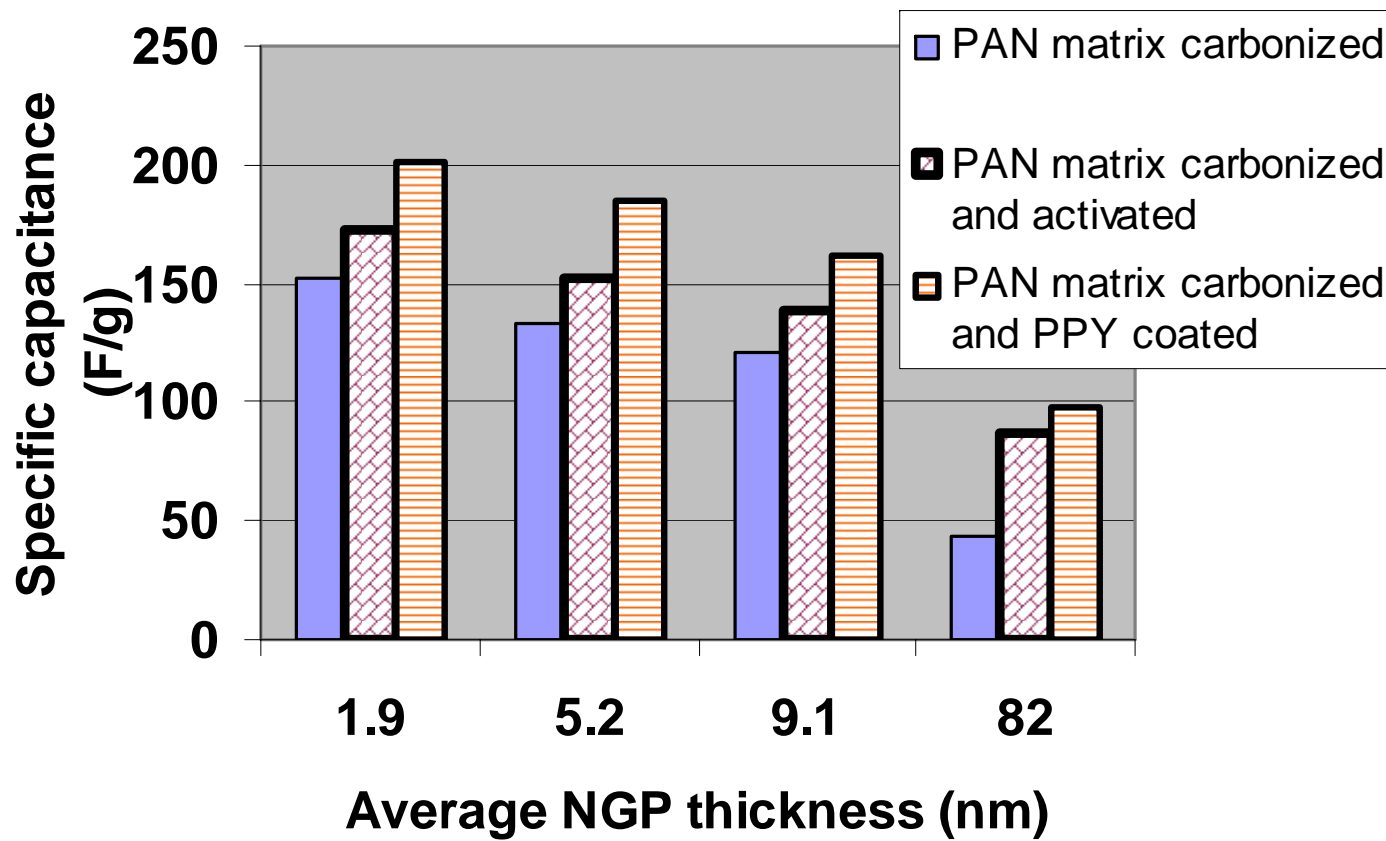


FIG.2

Fig. 3 Specific capacitance of NGP-based, PAN-derived meso-porous nanocomposites.



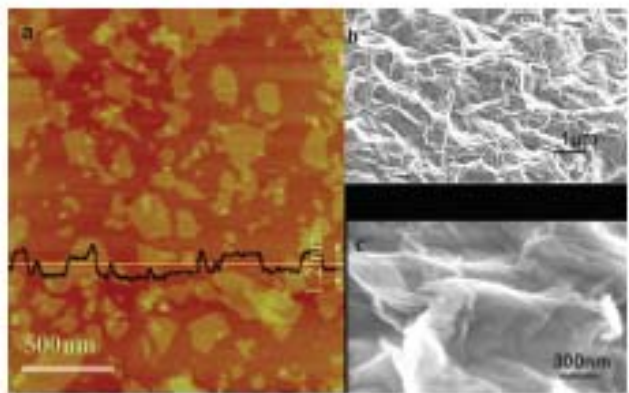


Figure 2. Morphology of graphene oxide and GMs. (a) Tapping-mode AFM image of graphene oxide and height profile plot showing the ~1.2 nm thickness for individual graphene oxide sheets. The sample was prepared by spin-coating the dilute graphene oxide dispersion (1.0 mg/mL) onto a freshly cleaved mica surface. (b, c) Scanning electron microscopy (SEM) images of GM-A with different scale bars.

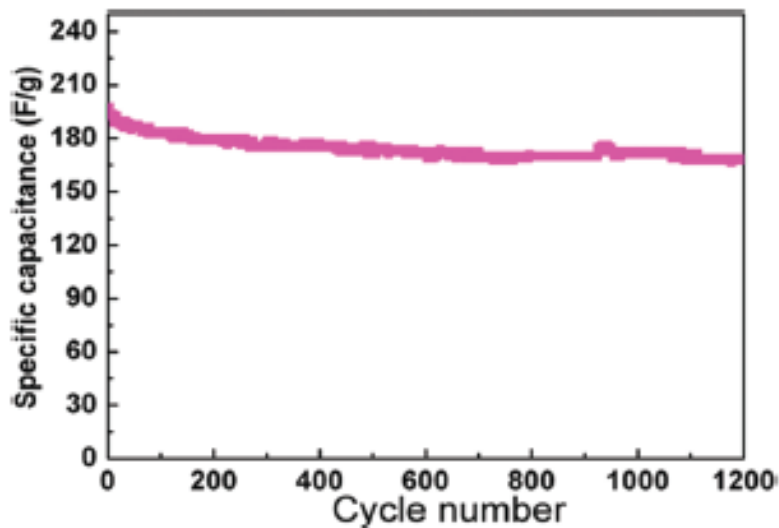


Figure 5. The specific capacitance change at a constant current density of 500 mA/g as a function of cycle number.

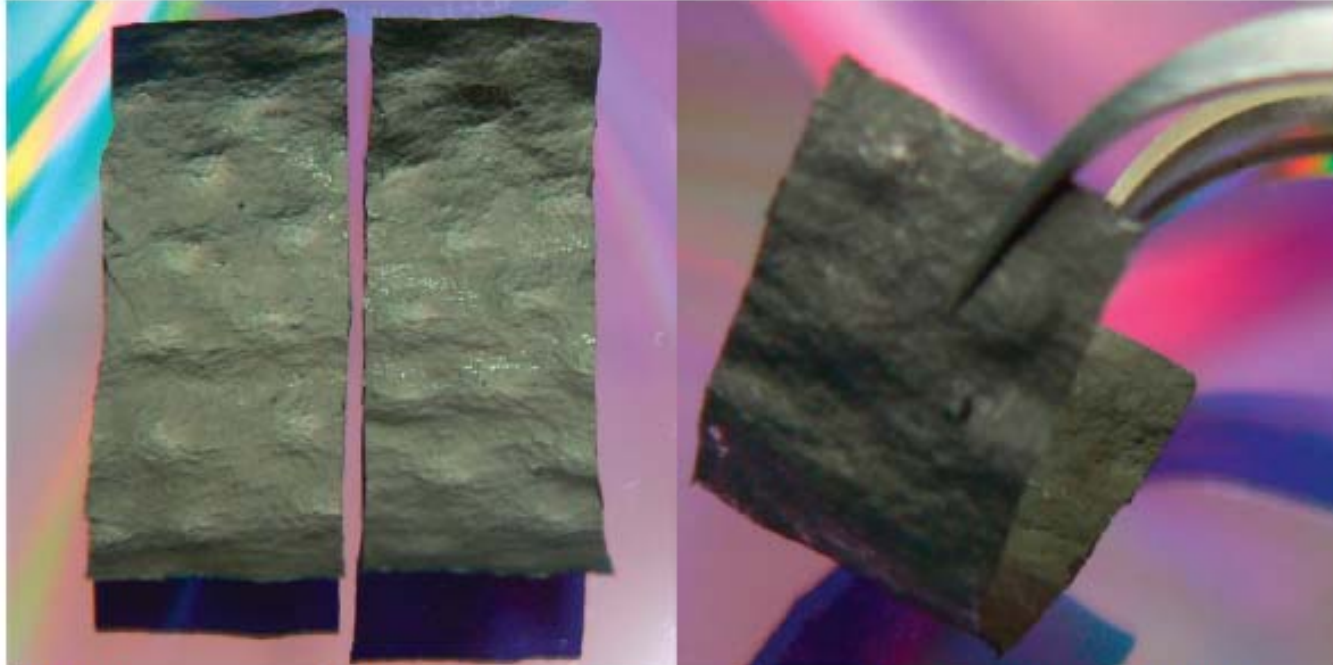


Figure 2. Digital camera images of (left) two freestanding G-papers (30 mm × 10 mm) and (right) a flexible G-paper.

ACS NANO

VOL. 3 • NO. 7 • WANG ET AL.

www.acsnano.org

233 F/g and 135 F/cm³

D. W. Wang, et al. ACS Nano, 3 (2009) 1745

Bipolar Plates



- The bipolar plate is one of the most costly components in a PEM fuel cell (typically amounting to 33% of the stack cost).
- Bipolar plates typically account for more than 80% of the weight and 95% of the volume of a fuel cell stack.
- Dictate the gravimetric and volumetric power density of a fuel cell stack.

Bipolar Plates

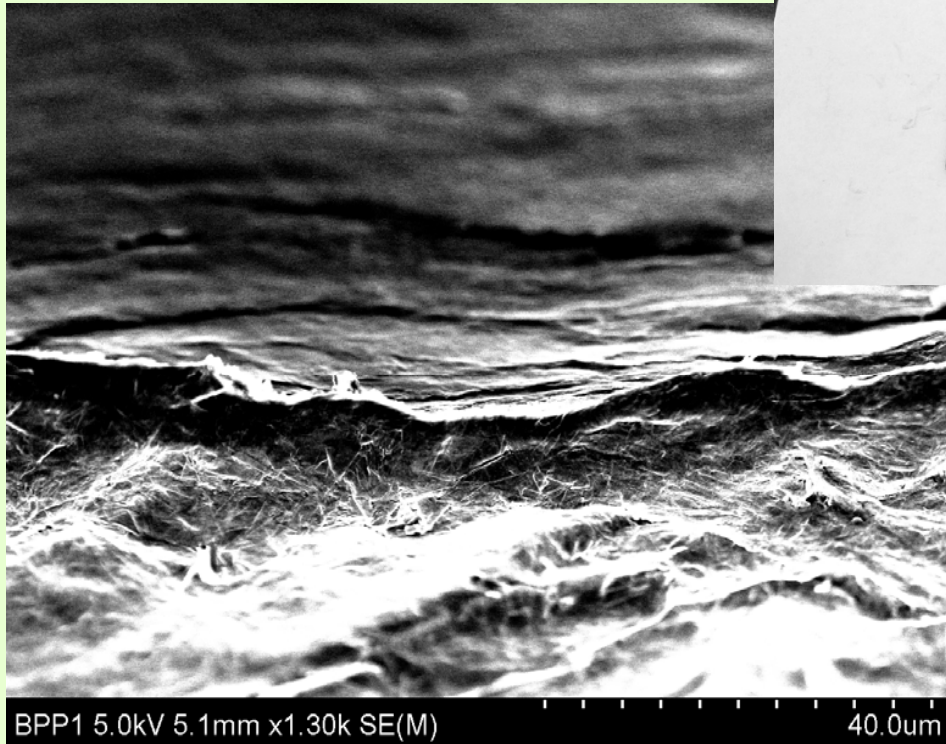
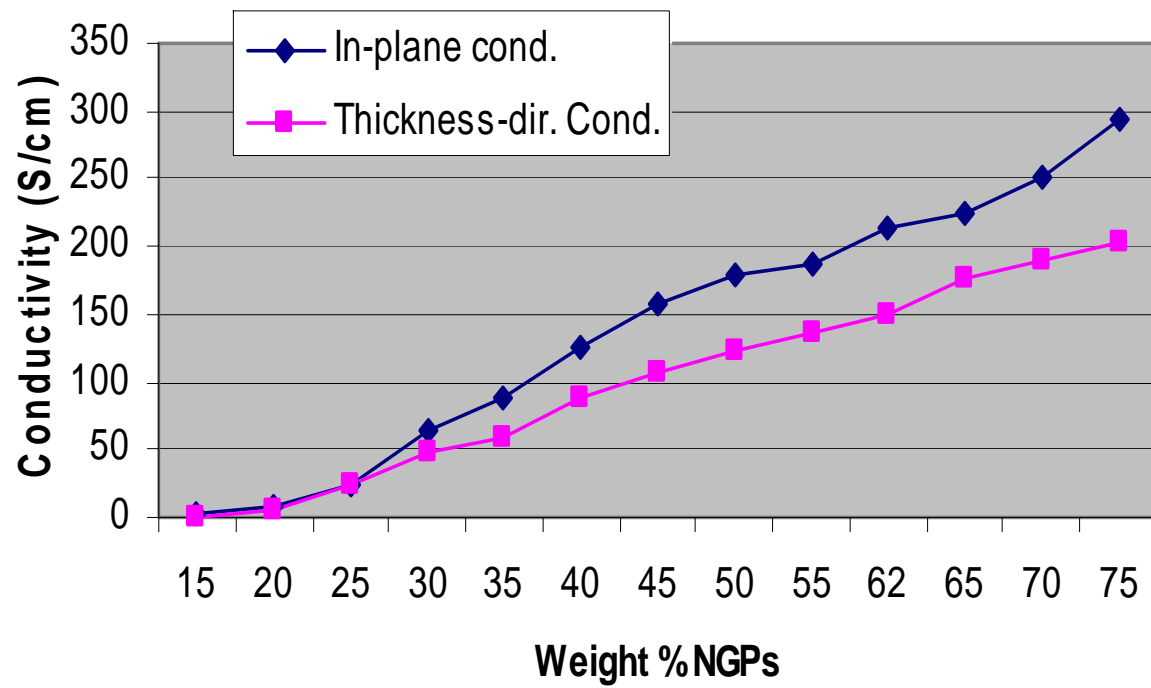


FIG.5(B) In-plane and through-plane conductivity of NGP composites.



Current Research Issues

- Production of large-area, defect-free single-layer graphene sheets for device applications.
- Functionalization of NGPs for nanocomposite applications.
- Experimental determination of mechanical, electrical, magnetic, and thermal properties of individual NGPs.
- Many unique properties (e.g. for energy applications) have yet to be discovered.

Thank you.

www.AngstromMaterials.com